THE JOURNAL OF THE AMERICAN CERAMIC SOCIETY, OCTOBER 1, 1944

THE JOURNAL

OF THE

AMERICAN CERAMIC SOCIETY

NOVEMBER 1, 1944

MONTHLY PUBLICATION DEVOTED TO THE ARTS AND SCIENCES RELATED TO THE SILICATE INDUSTRIES

Vol. 27, No. 10, pp. 285-316 (1944)

TABLE OF CONTENTS

Vol. 27 November 1, 1944 No. 11

THE JOURNAL

Particle Shape and Differential Shrinkage of Steatite-Talc Bodies 317–20
By Richard S. Lamar

Particle-Size Distribution of Steatite Talc 320–23
By J. S. White

Effect of Additions of Diopside on Properties of a Wall-Tile Body 324–26
By C. R. Amberg

Fusion Experiments in System $MgO–FeO–Cr_2O_3–Al_2O_3$ 327–29
By Henry N. Baumann, Jr.

Glass Stones 330–50
By W. L. Fabianic

Mechanics of Enamel Adherence: XVI, Influence of Manganese Dioxide on Metal Precipitation of Ground Coat-Iron Interface 350–51
By R. M. King

Observations Indicating Absence of Plastic Flow in Glass Coating on Steel 352–54
By W. G. Martin and F. W. Lauck

Publication Office: 20th & Northampton Sts., Easton, Pa.
Editorial Office: 2525 N. High St., Columbus 2, Ohio
Committee on Publications: R. L. Stone, *Chairman;* R. E. Birch, H. Z. Schofield, H. Thiemecke, and R. C. Purdy, *ex officio*

Entered as second-class matter at the post office at Easton, Pa., under the act of March 3, 1879. Published monthly
Subscription fifteen dollars ($15.00) a year. Single numbers $1.50
(Foreign and Canadian postage, 50¢ additional on subscriptions)
(Copyright 1944, American Ceramic Society, Inc.)

THE JOURNAL
OF
THE AMERICAN CERAMIC SOCIETY

Volume 27 | November 1, 1944 | Number 11

PARTICLE SHAPE AND DIFFERENTIAL SHRINKAGE OF STEATITE TALC BODIES*

By Richard S. Lamar

Abstract

An attempt has been made to correlate the differential shrinkage of fired steatite pieces with the particle shape of the raw talc used in their manufacture. Various talcs of widely varying particle shape were used in making the steatite test pieces. It was found that the more irregular in shape the talc particles, the greater the differential shrinkage.

A method is given for assigning arithmetical values to various particle shapes depending on their deviation from sphericity, this arithmetical value being known as specific shape factor. A direct relationship was found to exist between the differential shrinkage of a talc and its specific shape factor. As the talc particles became more irregular in shape, the "specific shape factor" value increased and the differential shrinkage was found to increase. The proper selection of the talc to be used and blends of various talcs were found to be helpful in the control of differential shrinkage.

I. Introduction

In the manufacture of steatite by the dry-press method as well as by the extrusion method, some talcs have been found to have a greater differential shrinkage† than others after firing. Tests made in this laboratory have shown that talcs of uniform granular particle shape have comparatively low differential shrinkage whereas those talcs of a fibrous, micaceous, or irregular particle shape have comparatively high differential shrinkage. It has also been found that differential shrinkage is relatively higher in extruded bodies than in dry-pressed bodies and that it increases with increased pressure in dry-pressed bodies. The differential shrinkage undoubtedly is caused by particle alignment, and there would logically be a greater change for alignment upon extrusion than upon pressing. With increased pressure, however, greater alignment occurs and differential shrinkage increases.

Each individual particle theoretically shrinks differently along its different axes, and the combined effect of each particle results in differential shrinkage. Particle alignment, moreover, causes a difference in bulk specific gravity within different portions of the piece, which would also have a marked influence on the shrinkage.

Various numerical values have been assigned in this work to different particle shapes depending on their relationship to spheres of equal volume or equal surface, the final result being a factor termed the "specific shape factor." This specific shape factor will be shown to be directly related to differential shrinkage, which varies directly as the specific shape factor varies.

II. Calculation of Specific Shape Factor

For any irregular-shaped particle, a hypothetical particle can be substituted which is spherical in shape and has the same volume or the same surface as the irregular-shaped particle. It would be possible, similarly, to substitute a hypothetical diameter for such a spherical particle or an average diameter for a distribution of irregularly sized and shaped particles. These average diameters are found to have values as shown in equations (1) through (5).

The specific surface for a particulate substance is the surface per unit weight or unit volume of the substance; therefore, the finer the material, the larger the specific surface. The specific surface (surface per unit weight) of a particulate substance can then be calculated by equation (6), if all of the particles are spherical in shape or are assumed to be spherical. Equation (6), how-

* Presented at the Forty-Sixth Annual Meeting, The American Ceramic Society, Pittsburgh, Pa., April 5, 1944, White Wares Division (supplementary title not listed). Received June 24, 1944.

† Differential shrinkage means the relationship between linear and diametrical shrinkage.

Mean diam. (length) $= d_l = \Sigma nd^2/\Sigma nd$ (1)

Mean vol. diam. $= d_v = \sqrt[3]{\Sigma nd^3/\Sigma n}$ (2)

Mean surface diam. $= d_s = \sqrt{\Sigma nd^2/\Sigma n}$ (3)

Mean vol.-surface diam. $= d_{vs} = \Sigma nd^3/\Sigma nd^2$ (4)

Wt. mean diam. $= d_w = \Sigma nd^4/\Sigma nd^3$. (5)

n = frequency of occurrence.
d = diam. of particles occurring in distribution of particles.

ever, will give only an approximate value in most cases because of the necessity of assuming the particles to be spherical.

$$S_w = 6/d_w P \quad (6)$$

S_w = surface per unit wt.
d_w = wt. mean diam. (as in equation (5)).
P = density of material.

The more irregular the particles, the greater will be the error in value for specific surface obtained in this manner; it is possible, therefore, to calculate only a hypothetical specific surface. This method consists of (1) determining the particle-size distribution of the material, (2) calculating a mean statistical diameter as described previously, and (3) from this, calculating a statistical specific surface based on the assumption that all of the particles are spherical. The specific surface of a substance consisting of irregular-shaped particles obtained in this manner will be low because for each individual particle in the material any deviation from sphericity would cause an increase in the surface of the particle and, similarly, an increase in surface for a unit weight or unit volume of the material, which is essentially the definition of specific surface.

If the actual or true specific surface of the material can be measured, this value will be related to the specific surface, based on the assumption that the particles are spherical by some factor which will be a measure of particle shape or, more properly, a measure of deviation from sphericity. If the particles are actually spherical, the statistical specific surface will be equal to the true specific surface. The more irregular in shape the particles, the greater will be the difference between actual and statistical specific surfaces. For example, if Sw is the statistical specific surface and Sw' is the true specific surface, equation (7) will result, and the shape factor for spherical surfaces is shown to be π.

$$Sw/Sw' = a_s/\pi \quad (7)$$
a_s = shape factor.

When S = surface, V = volume, a_s = shape factor, a_v = volume factor, d_s = mean surface diameter, and d_v = mean volume diameter for a particulate substance, equation (8) can be formulated.

$$V = a_v d_v^3 \text{ and } S = a_s d_s^2 \quad (8)$$

In the case of a sphere, $a_v = \pi/6$ and $a_s = \pi$. If there are N particles in a unit weight of a material of density, P, equations (9) and (10) can be formulated.

$$V = 1/PN = a_v d_v^3 \quad (9)$$

$$Sw = SN = 1/P \times a_s/a_v \times d_s^3/d_v^3 \quad (10)$$

With N particles of weight, w, and density, P, the mean diameter is given by equation (11).

$$d = (1/a_v)^{1/3} (w/N_P)^{1/3} \quad (11)$$

The surface of an average particle will be $a_s d_s^2$, which will give equation (12).

$$\text{Surface} = [a_s(1/a_v^2)^{1/3}] (w/N_P)^{2/3} = a_w (w/N_P)^{2/3} \quad (12)$$

The term within the brackets in equation (12) is a measure of particle shape and may be termed the specific shape factor of a particle. For spheres, the specific shape factor is 4.85; for irregular particles, it is usually greater than 6.0. Values ranging from 5.03 for uniform, granular-shaped talcs to 6.11 for micaceous talcs were obtained by the writer in this study.

Another means of defining irregular particles is by noting the value of the ratio of surface to volume factors, that is, by the variable, a_s/a_v. It has been shown that a_s/a_v is approximately 6.1 for rounded particles, 6.4 for worn particles, 7.0 for sharp particles, and 7.7 for angular particles. For spheres, $a_s/a_v = 6.0$. This ratio enters into the formula for specific surface. Values greater than 6.0 were obtained for each of the talcs tested, showing that none of these talcs was composed of truly spherical particles. The most spherical talc was the White Mountain talc (see Table I), having a shape to a volume constant ratio of 6.74. The least spherical was No. $2^1/_2$ A talc, which was composed of micaceous particles and which also had the largest differential shrinkage on firing. The ratio for this talc was 12.22, showing a great deviation from sphericity for this talc.

III. Data on Specific Shape Factor

Six talc specimens were chosen for the tests, each being selected for its particular particle shape. Particle-size distribution tests were made on each sample and a statistical specific surface value was calculated for each. The true specific surface of each sample was then determined by Carman's permeability method[1] and a shape and volume factor for each talc was calculated from these values of statistical and actual specific surface. The specific shape factor was then determined. Samples of each talc were formed into test pieces and fired at 2200°F., measured for linear and diametrical shrinkage, and the differential shrinkage was calculated. The specific shape factor was then plotted against differential shrinkage, and it was found that the more irregular the particles, the greater the specific shape factor and the greater the differential shrinkage.

The hydrometer method was chosen to determine the particle-size distribution of each talc. By this method, a suspension is made of the material to be tested. As settling takes place, changes in specific gravity at definite time intervals are observed by means of a sensitive hydrometer, and the particle-size distribution can be calculated. The accuracy of the method depends on the accuracy of determining a refer-

[1] P. C. Carman, "Determination of Specific Surface of Powders ,I," *Jour. Soc. Chem. Ind.* [London], **57** [7] 225–34 (1938); *Ceram. Abs.*, **18** [10] 274 (1939).

TABLE I

STATISTICAL DATA ON TEST TALC SAMPLES

Talc	Particle type	Specific surface (cm.²/gm.) Statistical (Sw)	Specific surface (cm.²/gm.) Permeability (Sw')	Shape factor (a_s)	Volume factor (a_v)	a_s/a_v	Mean diam. (dm)
Oasis	Semimicaceous	2.34×10^3	3.15×10^3	2.34	0.290	8.06	9.23
Fibrene "C"	Fibrous	3.15×10^3	4.29×10^3	2.30	0.281	8.19	6.78
No. $2^1/_2$ A	Extremely micaceous	1.05×10^3	2.14×10^3	1.54	0.126	12.22	20.24
Talc City Hi-Grade	Granular	1.87×10^3	2.13×10^3	2.76	0.404	6.84	11.71
White Mountain	Granular	2.10×10^3	2.36×10^3	2.80	0.415	6.74	10.35
CB ceramic No. 99	Semifibrous crystalline	1.515×10^3	1.785×10^3	2.66	0.376	7.08	13.90

Talc	Specific shape factor (a_{sw})	Shrinkage (%) Diametrical (D)	Linear (L)	Differential ($L - D$)
Oasis	5.34	2.98	5.14	2.16
Fibrene "C"	5.36	7.80	4.39	3.41
No. $2^1/_2$ A	6.11	0.11*	6.81*	6.70
Talc City Hi-Grade	5.05	4.64	4.36	0.28
White Mountain	5.03	2.38	2.40	0.02
CB ceramic No. 99	5.10	2.28	3.50	1.22

* Expansion occurred here.

ence point along the length of the hydrometer below which any change in density would not affect the hydrometer. This constant is called the "effective depth" and may be calculated by the use of equations (13), (14), and (15).

If L be the distance from the surface of the suspension to the volume center of the hydrometer and if the submerged part of the stem is neglected, equation (13) can be derived.

$$L = L_1 + {}^1/_2 (L_2 - V_B/A) \tag{13}$$

L_1 = distance from top of suspension to top of hydrometer bulb.
L_2 = length of hydrometer bulb.
V_B = volume of hydrometer bulb.
A = cross-section area of graduate.

Equation (14) is then formulated.

$$de = 0.175 \sqrt{\mu/P - P_0} \times \sqrt{L/t} \tag{14}$$

de = equivalent spherical diameter (mm.).
μ = viscosity of suspension (poises).
P = density of particles.
P_0 = density of fluid.
t = time (min.).
L = function of density.

The weight percentage of solids in suspension at depth L at time t is then calculated from equation (15).

$$C/100 = 1000/w \times P/P \times P_0 (v_0 - P_0) \tag{15}$$

C = wt. concentration of particles per unit volume.
w = wt. %.
v_0 = specific gravity of suspension at time t.

The statistical specific surface may be calculated from the particle-size distribution by equation (16).

$$Sw = \frac{K \times 10^2}{P} \Sigma n/d \tag{16}$$

Sw = specific surface (cm.²/gm.)
K = shape constant ratio (e.g., $a_s/a_v = K = 6$ for spheres).
P = density of material.
n and d = frequency (percentage) and mean diameter, respectively.

This method gives only a statistical specific surface, based on the assumption that all of the particles are spherical. The results obtained by this method were low. In order to obtain the true specific surface of each sample, Carman's permeability method[1] was used. This method has been found to hold true over quite large ranges in a change of particle shape and, for this reason, gives a much truer value of specific surface for irregular particles than does the statistical method based on particle-size distribution.

Carman's method is based on the Kozeny equation[2] (17).

$$q = \frac{kA\, v_w^3}{\mu(1 - v_w)^2} Sv^2 \times \frac{\Delta P}{L} \tag{17}$$

q = rate of flow through packing.
A = cross-section area.
v_w = voids per unit wt.
ΔP = pressure gradient.
L = depth of packing.

Carman defined permeability by use of equation (18). The value of K' was found to be 5.0 for most materials.

$$P' = \frac{q}{K'vSv^2} \times \frac{v_w^3}{(1 - v_w)^2} \tag{18}$$

$K' = 1/K$.
$v = \mu/P_0$.

Equation (18) can easily be put in the form of equation (19), from which it is possible to calculate the specific surface from the porosity and permeability of the sample.

$$Sw = 14/P_0 \sqrt{1/Pc'v \times v^3/(1 - v)^2} \tag{19}$$

For fibrous materials, the value of constant K' must be changed from 5.0 to 5.5. The evaluation of the porosity function, $v^3/(1 - v)^2$, is critical and must be determined to the utmost accuracy.

[2] Josef Kozeny, "Über Kapillare Leitung des Wassers im Boden (Aufstieg, Versickerung, und Anwendung auf die Bewässerung)," *Sitzb. Akad. Wiss. Wien. Math. naturw. Klasse*, **136, Abt. IIa,** 271–306.

IV. Value of Calculations

The results of this work lead to several definite conclusions as to the effect of particle shape on differential shrinkage. (1) Particle shape does control differential shrinkage; (2) differential shrinkage is not controlled by particle size, but particle size affects shrinkage; (3) generally, the more irregular the particles, the higher the specific shape factor and the greater the differential shrinkage of the particulate substance; (4) the various values for linear and diametrical shrinkage suggest that differential shrinkage can be largely controlled by blending talcs of different particle shape; (5) irregularity of shape toward the micaceous form usually causes greater differential shrinkage than the fibrous form; and (6) increased fineness or a change in particle-size distribution for each talc was found to have no material effect on the particle shape and therefore did not change the differential shrinkage.

It is interesting to note the high shape factor for the CB ceramic No. 99 talc (Table I). The differential shrinkage on this material is low, which in part bears out the high shape factor obtained. Many of the particles, although quite irregular as compared with spheres, were found to be rough rectangular parallelopipeds which act much like spheres.

Sample No. 2½ A talc is extremely micaceous and the particles appear to have a lamellar structure. The firing expansion is probably due to exfoliation; this, however, is not true of the Oasis talc. Table I shows statistical figures on each grade of the talc test samples.

Sierra Talc Company
Los Angeles, California

PARTICLE-SIZE DISTRIBUTION OF STEATITE TALC*

By J. S. White

Abstract

Experiments were made to determine which degree of fineness of ground talc would be most suitable for steatite-type ceramics. A laboratory-type air separator, Andreasen pipette, and the Casagrande hydrometer methods were used to measure the particle-size distribution of commercial steatite talcs.

The results indicate that, although wide variations in the particle-size distribution of steatite talcs have a bearing on the firing shrinkage when the talc is incorporated in a body, the differences in grinding obtained in commercial talcs are not of great importance when proper milling practice is employed.

I. Introduction

In the past, high-grade talc, such as that required for steatite manufacture, has been purchased on a basis of the percentage retained on a 200- or 325-mesh screen, possibly a carry-over from the experience of the talc producers in grinding for the cosmetic industry where the important specifications are "slip," color, and freedom from certain irritating impurities and grit. The experimental work discussed in this paper was carried out for the purpose of determining what degree of fineness might be most desirable for use in the manufacture of steatite ceramics.

II. Particle-Size Measuring Equipment

The measurements of particle-size distribution beyond 200-mesh were made chiefly by one of two methods. The first method employed, and the one chosen for most of the work, was the use of a laboratory-type air separator. With a given rate of air flow, a sample of the talc was separated into coarse and fine fractions, and the percentage of the original sample remaining in the coarse fraction was determined by weighing. The coarse fraction was selected in order to avoid errors that might be introduced by the difficulty in recovering all of the ultra-fine material from the dust-collecting bags. The exact size at which the separation was made was measured with a microscope equipped with a calibrated ocular. This method was felt to be more dependable than attempting to calibrate the separator in terms of the rate of air flow. Repeating with different rates of air flow made it possible to plot a particle-size distribution curve. The type of plot used was one showing cumulative percentage of material coarser than a given size, plotted on a linear scale, against that size expressed in microns, plotted on a logarithmic scale. The logarithmic scale was employed because it has the characteristic that any size ratio is always represented by the same distance on the particle-size axis.

Later curves were determined by means of the Andreasen pipette method in which the sample was dispersed in a liquid; the concentration of solid material in samples drawn off at a certain depth below the surface at various time intervals, was used to calculate the particle-size distribution by the application of Stokes' law. A few of the most recent measurements have been made by the Casagrande hydrometer method, which is basically similar to the Andreasen pipette method except that a hydrometer is used to determine, at various intervals, the density of the suspension at a fixed distance below the surface. This avoids the necessity of carefully drying and weighing a series of samples.

The air-separator method has several disadvan-

* Presented at the Autumn Meeting of the White Wares Division, The American Ceramic Society, Uniontown, Pa., September 17–18, 1943. Received May 4, 1944.

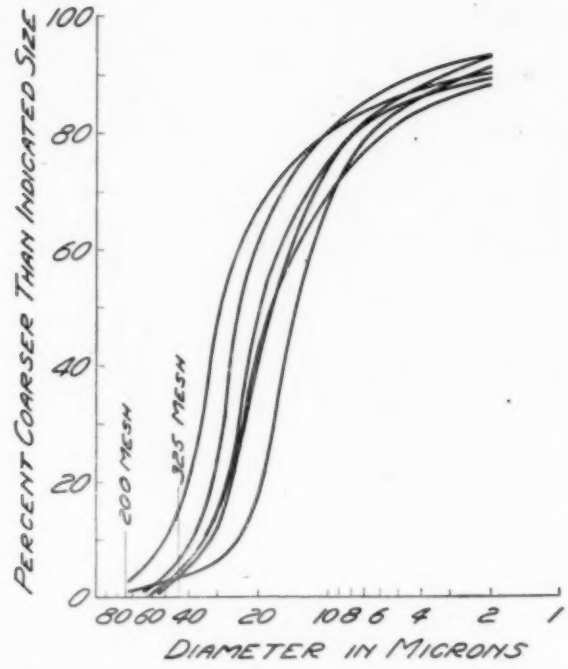

FIG. 1.—Particle-size distribution curves of six typical talcs.

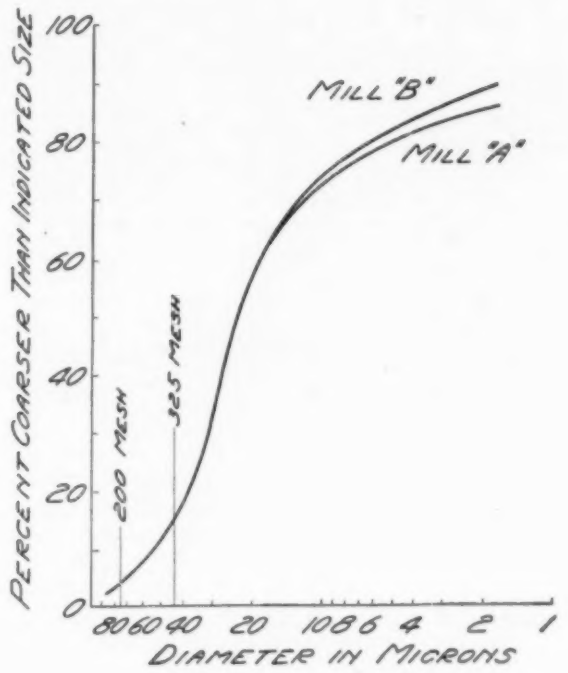

FIG. 2.—Comparison of particle-size distribution of talc ground in two plants.

tages. It requires a large sample for testing and is time-consuming, due to the number of samples which must be separated. In the case of talcs, an additional drawback is the necessity of running each sample repeatedly to avoid a considerable error caused by particles which clump together and act as a single large particle.

The two sedimentation methods, although requiring a comparatively long time to run, do not demand continuous attention and therefore consume less of the operator's time. If the proper deflocculant is used, no trouble is encountered from clumping of the particles. Of these two sedimentation methods, the hydrometer method is probably better for routine checking of particle size, since the equipment for running a number of simultaneous tests is less costly and the necessity of making a large number of time-consuming analytical balance weighings is avoided. Some uncertainty, however, arises from the disturbance of the settling column by the introduction of the hydrometer and also from the fact that the hydrometer does not actually measure the density of the suspension at a fixed depth but rather an average density over a range of depths inasmuch as the hydrometer bulb occupies a considerable amount of space.

III. Comparison of Commercial Talcs

Figure 1 shows typical particle-size distribution curves obtained from six different talcs. Four of the talcs were obtained from the California district and were ground in Raymond-type mills. One, specially selected for low tremolite content, was from New York State and was ground in a tube or ball mill. The sixth was from Manchuria, ground in an unknown type of

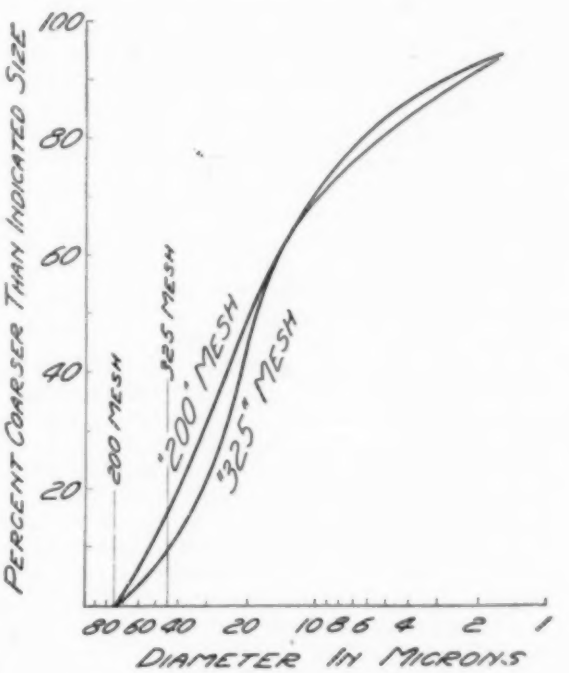

FIG. 3.—Comparison of particle-size distribution of so-called "200-mesh" and "325-mesh" talc.

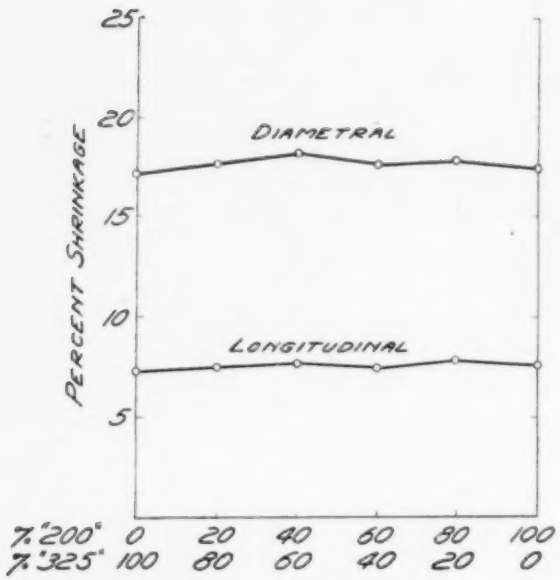

FIG. 4.—Effect of substitution of "200-mesh" talc for "325-mesh" talc on shrinkage of a talc-clay body (total talc 84%, ball clay 16%).

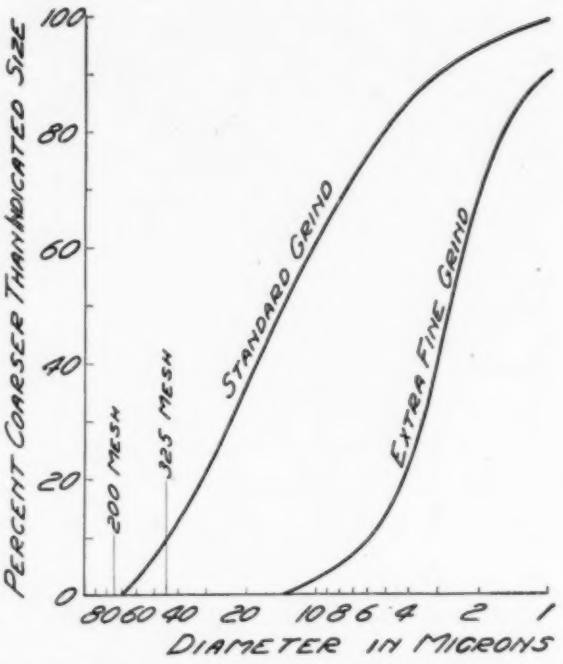

FIG. 5.—Particle-size distribution curves of standard grind and extremely fine grind talc.

mill, probably in Japan. The differences in particle-size distribution between the various talcs were not particularly great as the composite curves show. The sizes corresponding to 200-mesh and 325-mesh, marked on the particle-size axis, show the inadequacy of screen sizes as an indication of the degree of fineness of talc.

Figure 2 shows the particle-size distribution obtained on two samples of talc, both from the same deposit but ground in two different plants of the same supplier. The two curves are quite similar except for a slight difference at the extreme fine end. This similarity is evidence that it is possible for millers to grind talc to similar particle-size distribution in successive lots even though it may not be done in exactly the same mill, but it does not mean that a change in the material fed to the mill, arising from changes in the sorting of the crude talc, will not affect the particle-size distribution. It does indicate, however, that the mill operation itself can be controlled with sufficient accuracy to insure a uniform material.

Figure 3 shows the particle-size distribution for samples of a talc, ground to two specifications, namely, "325-mesh" and "200-mesh." It will be seen that the difference is very slight, the finer material being approximately what would be obtained if about 8% of +325-mesh material were removed from the coarser. The amount of shrinkage of these two lots of talc when incorporated into a vitreous extruded test body was virtually the same (see Fig. 4), and there was no noticeable difference in the texture or porosity of the test bodies. This suggests that it may be possible to lower the cost of talc for ceramic purposes by using a coarser grind than that which has become standard for the cosmetic trade. This, of course, would be of more importance in the cheaper grades of talc because the grinding cost for such grades is a greater portion of the total cost. The limit to which this grinding could be carried would, of course, be determined by the size which would begin to cause inhomogeneity in the body. This stage had definitely not been reached with the coarser of the two materials tested.

IV. Effect of Extra Fine Grinding on Body Shrinkage

In order to test the effect of a fineness considerably beyond that of the usual grinds, a sample of the superfine material collected in the "bag house" of the talc mill during the grinding of a lot of talc was obtained for comparison with the standard grind produced at the same time.

Figure 5 shows the particle-size distribution of the standard grind and of the superfine material. The superfine material would be approximately 1000-mesh material if the Tyler-screen series could be extended. This size has approximately the same relation to 200-mesh as 200-mesh does to 28-mesh.

This material was incorporated into a series of test bodies composed of 84% talc and 16% ball clay with the superfine material replacing varying proportions of the standard talc up to 100% of the talc content. The bodies were prepared for extrusion with a constant small amount of organic binder and a constant percentage of mixing water and were extruded in a cylindrical column approximately one inch in diameter. The dried samples were fired together at a temperature which resulted in a moisture absorption of less than 0.05% for all of the samples. The percentage of shrinkage of the

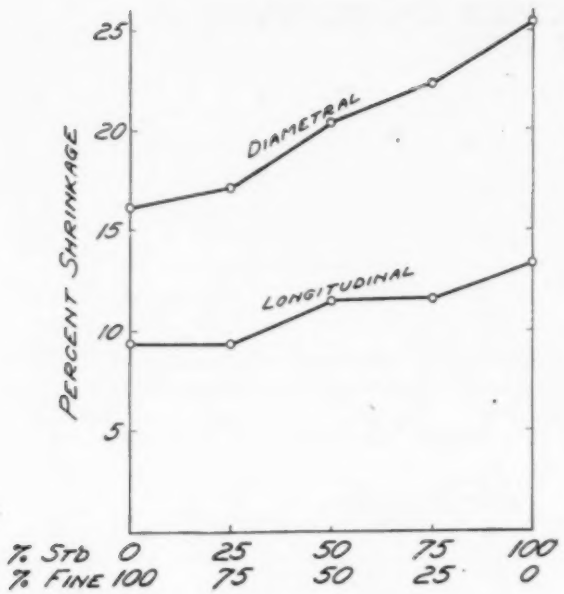

FIG. 6.—Shrinkage of test body with substitution of extremely fine talc for standard-size talc.

series of bodies is shown in Fig. 6. It will be seen that, for a large difference in particle size, the effect of the shrinkage is appreciable.

In the extrusion of talc bodies, the high ratio of diametral shrinkage to longitudinal shrinkage is a source of considerable trouble, causing distortion of shapes machined in the ware. For example, round holes that were drilled in green extruded stock at right angles to the direction of extrusion will be oval after firing. It might be thought that extremely fine grinding of the talc would have some effect on this "differential shrinkage." The shrinkage data shown in Fig. 6, however, indicates that any such effect is very slight, the ratio of the two shrinkages remaining practically constant for the whole series of bodies. This result should not be altogether unexpected, inasmuch as the differential shrinkage is probably due to alignment of the elongated or platelike talc particles as they flow through the extrusion die. Finer grinding of the talc should not change the relative shape of the particles, which is dependent on the natural cleavage characteristics of the mineral.

The use of the dust-collector fines in the foregoing work is open to some question for it allows the possibility that there has been a preferential selection of some part of the talc in the separation, leading to a difference in actual composition of the two grades of talc. This possibility was checked by a similar experiment in which the shrinkage of a standard grind talc was compared with that of the same talc which was ground in such a manner that the whole sample was completely reduced to the finer size. Results in this test were similar to those obtained when dust-collector material was used.

V. Summary

These tests indicate that, although particle-size distribution in steatite talcs has a bearing on the firing shrinkage when the talc is incorporated in a body, the differences in grinding normally found in commercial talcs are not of great importance. If extremely close control of the particle-size distribution of a certain talc is thought to be necessary, it can be attained by the talc producer. There are indications that coarser grinding may be advantageous for ceramic users from a cost standpoint and may be used without entailing radical changes in shrinkage. There appears to be no change in the ratio of diametral to longitudinal shrinkage in extruded bodies attributable to the particle size of the talc.

STUPAKOFF CERAMIC & MANUFACTURING COMPANY
LATROBE, PENNSYLVANIA

EFFECT OF ADDITIONS OF DIOPSIDE ON PROPERTIES OF WALL-TILE BODY*

By C. R. Amberg

Abstract

Diopside was substituted for both talc and feldspar in a typical wall-tile body. It was found to lower the fusion temperature and to lower thermal expansion when compared with talc and to raise thermal expansion when compared with feldspar. Its effects on firing shrinkage, fired absorption, and moisture expansion were somewhat similar to those of talc.

I. Introduction

In northern New York State, large quantities of a white diopside occur in deposits from which it is easily obtained by open-pit methods. It is contaminated with a little quartz and graphite, which are sufficiently segregated to permit removal by sorting. Theoretical diopside has the formula $CaO \cdot MgO \cdot 2SiO_2$, but this particular material contains an appreciable amount of alumina and a small amount of iron.

A program of experimental work to search for uses of this diopside in ceramics has been started at the New York State College of Ceramics, and material from some of the preliminary investigations is given in this paper. It was hoped, among other possibilities, that diopside might serve much the same purpose as talc in a wall-tile body.

II. Experimental

A series of bodies was prepared from compositions given in Table I and Fig. 1. These bodies were blunged, lawned, and dried in lined plaster bats. Dry-press bodies containing 8% of water were prepared, tempered, and disintegrated to pass a 28-mesh screen, and the test specimens were pressed at 2000 lb. per sq. in. Draw trials were made at a series of temperatures for shrinkage and absorption measurements. The pyrometric cone equivalent values were obtained, and thermal-expansion measurements were made on selected samples by means of the interferometer. The samples used for expansion measurements were those of the four end members of the blending diagram, fired at temperatures to produce approximately 10% absorption. The actual firing temperatures and absorptions are given in Table II.

Tile, pressed on a screw press, were fired at selected temperatures, glazed with a cone 1 glaze, and glost fired. These specimens were subsequently given an autoclave treatment of 150 lb. for one hour. It was intended to secure bodies with absorptions of the order of 10%. The screw press, however, evidently produced lower forming pressures than that of 2000 lb. per sq. in. used for the draw trials with the result that absorptions were higher than expected. The actual figures for this property in the tile used for glazing as well as the results on moisture expansions are given in Table IV.

The following frit and glaze formulas were used:

Frit formula

PbO	0.455			SiO_2	1.82
KNaO	0.182	Al_2O_3	0.10	B_2O_3	0.91
CaO	0.364				

Glaze formula

PbO	0.25			SiO_2	2.50
KNaO	0.25	Al_2O_3	0.30	B_2O_3	0.50
CaO	0.50				

Bar specimens, also made on the screw press, were autoclaved for one hour at 150 lb. per sq. in., and the percentage moisture expansion was determined by

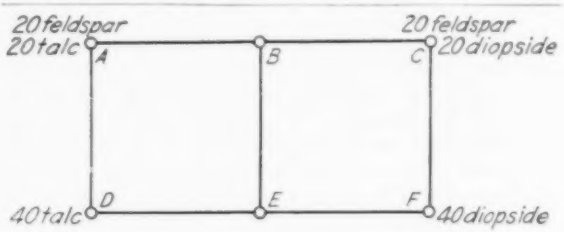

Fig. 1.—Test body compositions (see Table I).

Table I

Test Body Compositions (see also Fig. 1)

	Body					
	A	B	C	D	E	F
Old Mine Ky. No. 4 ball clay	12	12	12	12	12	12
Champion Challenger ball clay	10	10	10	10	10	10
Edgar plastic kaolin	15	15	15	15	15	15
Vanderbilt pyrophyllite	23	23	23	23	23	23
N. Y. tremolitic talc	20	10	0	40	20	0
Burnham diopside	0	10	20	0	20	40
Buckingham feldspar	20	20	20	0	0	0

Table II

Firing Temperatures and Absorption Data on Test Bodies

Body	Cone No.	Fired absorption (%)
A	$2^1/_2$	7.2
C	02	10.0
D	8	9.9
F	6	10.5

* Presented at the Forty-Sixth Annual Meeting, The American Ceramic Society, Pittsburgh, Pa., April 5, 1944 (White Wares Division). Received May 3, 1944.

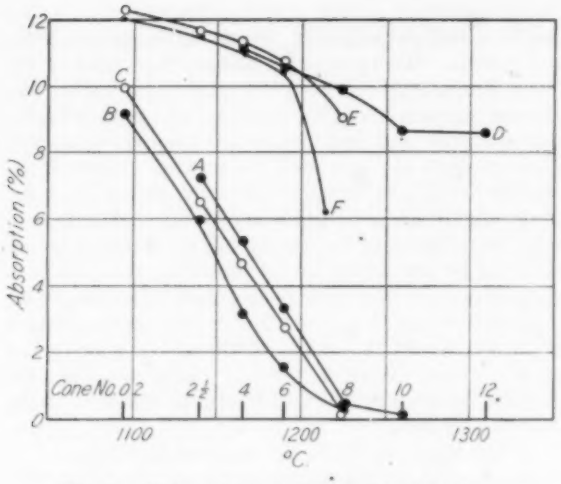

Fig. 2.—Firing characteristics of test bodies.

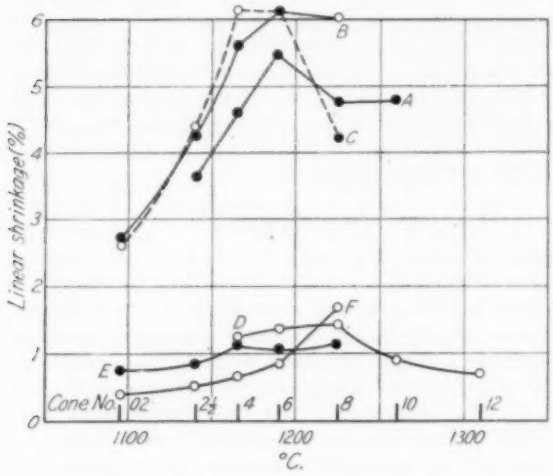

Fig. 3.—Firing characteristics of test bodies.

micrometer measurements. The results on these specimens also appear in Table IV.

III. Results

The P. C. E. values of the bodies were as follows: Body A cone 11½, B 10, C 9, D 14, E 8, and F 8. The bending interval was very short in all cases. The substitution of talc for feldspar raised the P. C. E., but it was lowered by the substitution of diopside for either talc or feldspar.

The firing characteristics of the bodies are shown in Figs. 2 and 3, where it is evident that the feldspar-bearing bodies have greater shrinkages and can be fired to lower absorptions without too much danger of complete fusion of the body. The substitution of either talc or diopside for feldspar, in general, produced bodies of low-firing shrinkage and high absorption. The substitution of diopside for talc in the feldspar bodies tended to increase the shrinkage slightly and to decrease the absorption. The substitution of diopside for talc tended

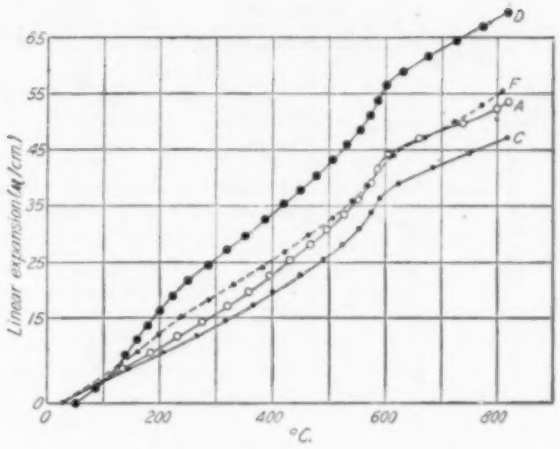

Fig. 4.—Thermal expansion data on test bodies.

to decrease slightly both shrinkage and absorption in the bodies containing no feldspar.

The color of the bodies was adversely affected by the diopside. All bodies had an ivory color at the lower temperatures; at the higher temperatures, the diopside produced a grayish body with an olive tint in the draw trials and a buff color in samples that were cooled with the kiln. This color would naturally set some limitations on the use of diopside in the bodies. The color apparently is caused by an iron-bearing phase which separates from solid solution in the diopside at about 1200°C. Inasmuch as the iron does not exist as a separate mineral, there is no hope of separating it from the raw diopside.

The thermal-expansion data on bodies A, C, D, and F show some interesting effects (Fig. 4). Body A shows a fairly straight-line expansion at the lower temperatures with a distinct quartz inversion at 575°C. and a lower expansion thereafter. When the talc is substituted for the feldspar (body D), a hump produced by cristobalite or tridymite appears in the region between 100° and 200°C. and a greater over-all expansion of the body occurs. Some quartz is still present as indicated by the hump at 575°C. This presence of tridymite and cristobalite explains the permanent expansion shown in Fig. 3 for body D. The tridymite and cristobalite are probably derived chiefly from silica freed by the decomposition of the clay and pyrophyllite.

When diopside is substituted for feldspar (body F), a similar phenomenon takes place, but the humps for both quartz and cristobalite are much less pronounced and the increase in over-all expansion is considerably less. The silica minerals apparently had entered into a glassy phase to a large extent.

When diopside is substituted for talc, a distinct lowering of the over-all thermal expansion takes place. In the feldspar-free bodies, the silica inversion humps are markedly reduced.

The lowering of expansion when a high-limed material is substituted for a high magnesia was unexpected, but with similar degrees of vitrification, the effect in these bodies is pronounced. Further confirmation of

TABLE III

RESULTS OF GLAZE TRIALS

Body	Cone	Crazing: Before autoclaving	Crazing: After autoclaving
A	02	Slight	Severe
A	5	"	"
B	02	Moderate	"
B	5	Severe	"
C	02	"	"
C	5	"	"
D	5	None	None
D	$8^1/_2$	"	Moderate
E	5	"	None
E	$8^1/_2$	"	Moderate
F	$6^1/_2$	"	Slight
F	$8^1/_2$	"	"

TABLE IV

PERCENTAGE ABSORPTION AND MOISTURE EXPANSION ON BODIES FIRED AT DIFFERENT P. C. E.

Body		Cone No. 04 (%)	02 (%)	5 (%)	$6^1/_2$ (%)	$8^1/_2$ (%)
A	Absorption	19.8	17.2	9.8		
	Moisture expansion	0.1	0.05	<0.01		
B	Absorption	21.5	16.3	8.8		
	Expansion	0.1	0.05	0.02		
C	Absorption	19.0	16.3	9.0		
	Expansion	0.08	0.06	0.04		
D	Absorption			18.5		18.3
	Expansion			0.03		0.03
E	Absorption			21.1		19.3
	Expansion			0.03		0.03
F	Absorption			18.3	17.8	5.3
	Expansion			0.04	0.03	<0.01

this tendency is illustrated by the glazed tile before autoclaving as is shown by bodies A, B, and C in Table III.

The effect of the low thermal expansion of body A appears as a slight crazing, and the still lower expansion of bodies B and C show progressively increased severity of crazing. The higher expansions of bodies D, E, and F result in no trace of crazing.

In the autoclave test, all of the feldspar-bearing bodies exhibited severe crazing, whereas the bodies free from feldspar showed either no crazing or markedly less crazing. With the latter bodies, those fired at the lower temperatures showed less crazing even when the absorptions were about the same as those fired at higher temperatures and only those containing some talc came through the test with no crazing. Because the moisture expansion, given in Table IV, was of much the same order of size in bodies with high talc and high diopside, the absence of crazing in the talc-bearing bodies can best be accounted for by assuming that the high thermal expansion of these bodies placed the glaze under a greater degree of compression so that more moisture expansion would be needed to throw the glaze under tensile stress. With a properly designed glaze, the diopside bodies would probably also be resistant to the autoclave crazing.

As was to be expected, the moisture expansion of all bodies decreased with decreasing absorptions, but with corresponding absorptions, the feldspar-containing bodies showed higher moisture expansions. The substitution of diopside for talc in these bodies tended to produce bodies with higher moisture expansion.

In the feldspar-free bodies, no difference in moisture expansion occurred when the talc was partially replaced by diopside and, in bodies of similar absorption, a slight increase in moisture expansion was experienced when diopside entirely replaced talc.

IV. Summary

The New York State diopside produces the following effects in the wall-tile bodies: (1) P. C. E. values are lowered when diopside is substituted for either feldspar or talc; (2) diopside produces effects similar to talc on the absorption and shrinkage of the bodies; (3) diopside has the disadvantage of producing a buff color when used in large quantities at higher temperatures; (4) the thermal expansion is lowered when diopside is substituted for talc and it is increased when substituted for feldspar; (5) the moisture expansion is lowered when diopside is substituted for feldspar but is not quite so satisfactory in this respect as talc; (6) the tendency of a glaze to craze both before and after autoclaving is diminished when diopside is substituted for feldspar but it is not as effective as talc in this respect.

RESEARCH DEPARTMENT
NEW YORK STATE COLLEGE OF CERAMICS
ALFRED, NEW YORK

FUSION EXPERIMENTS IN SYSTEM MgO–FeO–Cr_2O_3–Al_2O_3*

By Henry N. Baumann, Jr.

Abstract

Various methods have been suggested and tried for modifying chrome ores for refractory use. Chrome ores vary widely in chemical composition but are made up chiefly of MgO, Al_2O_3, FeO, and Cr_2O_3 combined as a member of an isomorphous spinel-type series. The problem of modifying chrome refractories by chemical and thermal treatment therefore involves a knowledge of the system MgO–FeO–Cr_2O_3–Al_2O_3. The present study is based on experiments in which two series of chromium oxide-alumina fusions containing 10% and 30% Cr_2O_3, respectively, were fused in an electric-arc furnace with MgO up to 5% and with FeO up to 5%. The determination of the effect of silica and titania on the primary crystallization of these fusions, as indicated by a petrographic method of examination, was the chief purpose of this work.

I. Introduction

Among the natural sources of oxides that can be fabricated into refractory products, the only commercial source containing chromic oxide is chrome ore. Perhaps no other source of refractory oxides is so variable or complicated in chemical and physical composition. Although the mineral composition of chrome ore is often simply called chromite ($FeCr_2O_4$), actually it is known that the iron is often replaced in part with magnesium and the chromium in part with aluminum. This isomorphous mineral, which may be given the molecular formula $((Fe,Cr,Mg)O\cdot(Cr,Fe,Al)_2O_3)$, is always associated with more or less accessory minerals that vary widely in amount and composition depending on the origin of the chrome ores. As shown by Seil,[1] these associated minerals often consist of one or more of the magnesium silicates, sometimes contaminated with smaller amounts of other elements.

The thermal study of any combination of the oxides that form chrome ores or, perhaps, the result of treating chrome ores is therefore important. The phase-rule diagram of the system MgO–Al_2O_3–SiO_2 and its included binary system have been established for some time.[2] Wilde and Rees[3] more recently have studied the system MgO–Al_2O_3–Cr_2O_3. The results of their work gave only a partial solution of the constitution diagram, owing to the difficulty of studying phase-rule relationships in complicated oxide systems of this order of refractoriness. In working with chrome ores from various sources, the amount of alumina dissolved by the spinel component of the fusion was found to differ widely, depending largely on small variations in the silica content of the ore.

In order to define more clearly the effect of these variables, the writer worked with natural ores and commercial oxides and also conducted experiments, using technically pure oxides, definite proportions of which were fused electrically. The results of these experiments are incorporated in a patent[4] covering a fusion-cast refractory composition high in chrome corundum.

II. Method of Preparation and Examination

The fusions were made in a small electric arc furnace, using 1-in. graphite electrodes and 10-lb. batches of technical-grade oxides in the proportions shown later. The fusion took place rapidly, and the electrodes were so manipulated that there was no reduction to metal. The batches were completely fused, and the resultant fusions were rapidly cooled in place. These fusions are believed to be representative of the composition and structure characteristic of equilibrium conditions not much below the liquidus of each composition fused. That this equilibrium near the liquidus was in general obtained was indicated in the case of magnesia-alumina-chrome oxide fusions by comparison with the established system MgO–Al_2O_3, where the composition approximated established conditions. For example, this fusion, which approximated the Rankin and Merwin[2] composition of MgO 5% and Al_2O_3 95% (10% of the Al_2O_3 was replaced with Cr_2O_3 in the present study) gave a phase relationship of spinel-alumina solid solution to alpha-alumina very close to that shown by the Rankin and Merwin diagram, as indicated in Fig. 4; the writer is therefore quite sure that the high-temperature equilibrium was maintained.

Wilde and Rees[3] found that the magnesia-spinel solid solution of alumina is unstable at lower temperatures, a fact the writer had independently observed when heat-treating spinel-alumina solid solutions at 1400°C.

In the present study, it is believed that the rate of cooling was too rapid for dissociation of the spinel-alumina solid solution.

Petrographic thin sections were made of a number

---

* Presented at the Forty-Sixth Annual Meeting, The American Ceramic Society, Pittsburgh, Pa., April 5, 1944 (Refractories Division). Received April 5, 1944.

[1] G. E. Seil, "Refractories from a Metallurgical Viewpoint," *Ind. Heating*, **2** [9] 517–21, 538–40; [10] 587–90; [11] 651–53; [12] 713–17 (1935); *Ceram. Abs.*, **15** [3] 94 (1936).

[2] G. A. Rankin and H. E. Merwin, "System MgO–Al_2O_3–SiO_2," *Amer. Jour. Sci.*, [4th Series], **45**, 301–25 (1918).

[3] W. T. Wilde and W. J. Rees, "Ternary System MgO–Al_2O_3–SiO_2," *Trans. Brit. Ceram. Soc.*, **42** [7] 123–55 (1943).

[4] R. C. Benner, H. N. Baumann, Jr., and G. J. Easter, "Refractory and Abrasive Material and Process of Making," U. S. Pat. 2,279,260, April 7, 1942; *Ceram. Abs.*, **21** [6] 126 (1942).

TABLE I

RESULTS OF PETROGRAPHIC EXAMINATION OF FIRST SERIES

PART I: Fusions made in 10-lb. lots; alumina-to-chromic oxide ratio kept constant at Al_2O_3 90% to Cr_2O_3 10%

Composition (%)		Percentage of each constituent: Anisotropic >1.740	Isotropic	Anisotropic <1.740	Opaque
MgO 5		47	53		
MgO 3		59	41		
MgO 1		95	5		
MgO 5	SiO_2 3	52	48		
MgO 5	SiO_2 2	84	16		
MgO 5	SiO_2 1	83	17		
MgO 3	SiO_2 3	84	16		
MgO 3	SiO_2 2	88	12		
MgO 3	SiO_2 1	89	11		
MgO 1	SiO_2 3	79	21		
MgO 1	SiO_2 2	87	13		
MgO 1	SiO_2 1	95	5		
MgO 5	TiO_2 3	61	37		2
MgO 5	TiO_2 2	55	41	4	
MgO 5	TiO_2 1	49	51		
MgO 3	TiO_2 2	88	8	3	1
MgO 1	TiO_2 2	81	11	7	1
MgO 5	FeO 5	56	32	12	
MgO 5	FeO 3	72	27	1	
MgO 5	FeO 1	65	33	2	
MgO 3	FeO 5	69	29	1	1
MgO 3	FeO 3	76	21	1	2
MgO 3	FeO 1	76	14		
MgO 1	FeO 5	90	6	2	2
MgO 1	FeO 3	89	8	3	
MgO 1	FeO 1	96	3	1	

PART II: Fusions made in 10-lb. lots; alumina-to-chrome oxide ratio constant at Al_2O_3 70% to Cr_2O_3 30%

Composition (%)		Percentage of each constituent: Anisotropic >1.740	Isotropic	Anisotropic <1.740	Opaque
MgO 5		61	39		
MgO 3		76	41		
MgO 1		79	21		
MgO 5	SiO_2 3	81	19		
MgO 5	SiO_2 2	82	18		
MgO 5	SiO_2 1	73	27		

of fusions, and the primary or at least chief crystalline phase was generally chrome-corundum.

The method of determining the percentage of the different crystalline phases in the various samples was by means of petrographic examination of powders. The sample was powdered to 200-mesh and finer in a Diamond mortar, sieving being done frequently so as to produce a minimum of fines. The measurement consisted in making an actual count of the percentage area occupied by the chrome-alumina crystals, spinel, and miscellaneous constituents. The counting was done by means of an ocular net grating. The powder was immersed in an oil having a refractive index, n = 1.740. (*a*) Isotropic material was chiefly spinel or glass of eutectic composition; (*b*) anisotropic material > 1.740 was chiefly chrome-corundum, which could also be identified by its purple color and its dichroism; (*c*) anisotropic material < 1.740 was negligible or small in amount in most cases, and when it was sufficient in

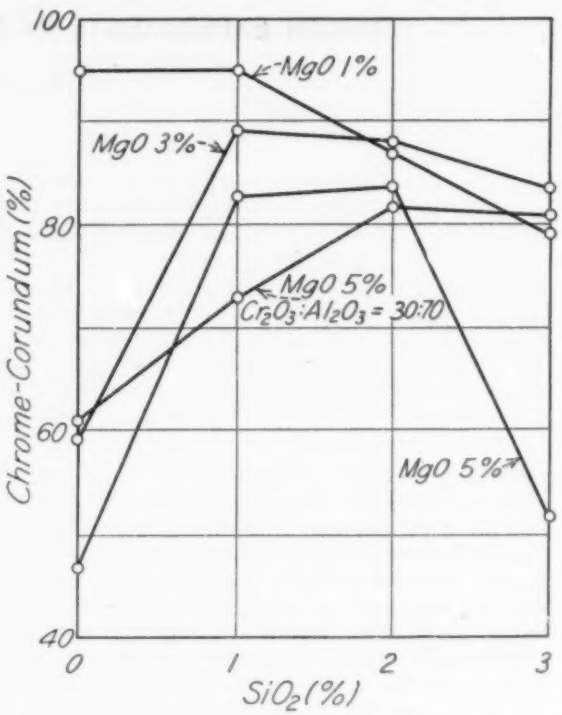

FIG. 1.—Effect of varying MgO and SiO_2 on amount of Cr_2O_3-Al_2O_3; the ratio of Cr_2O_3 to Al_2O_3 is 10 to 90, except as indicated.

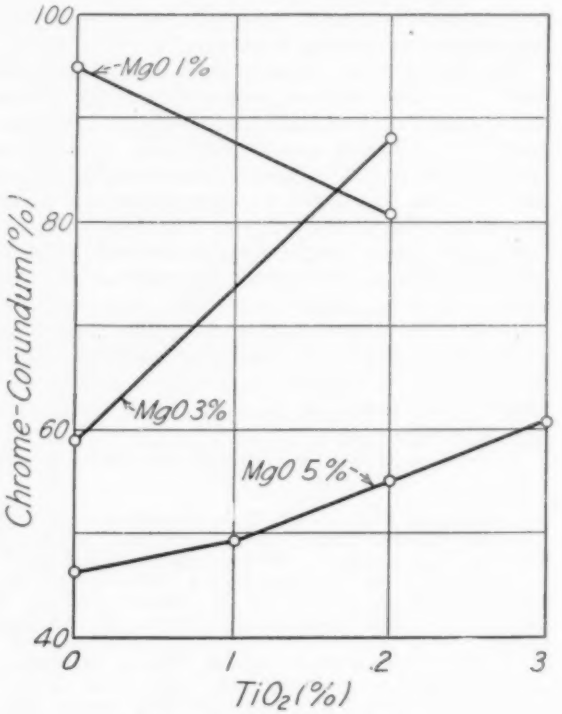

FIG. 2.—Effect of adding TiO_2.

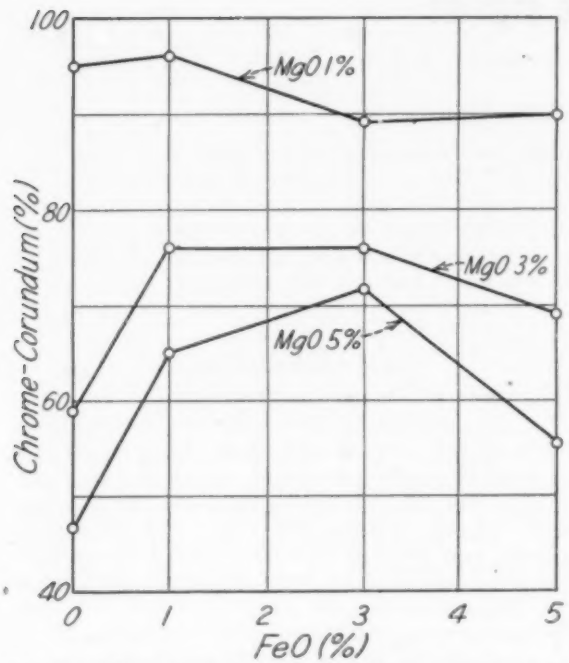

FIG. 3.—Effect of varying FeO and MgO on Cr_2O_3–Al_2O_3 (1:9) content.

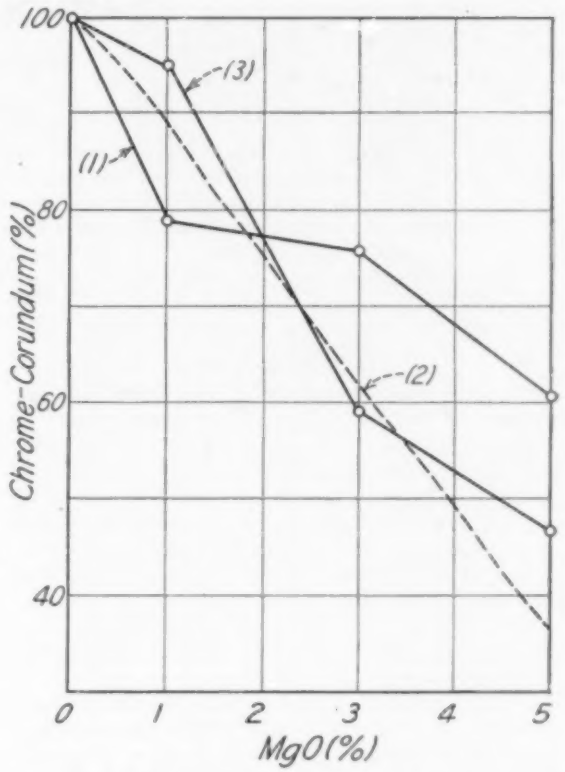

FIG. 4.—Effect of varying Cr_2O_3 and MgO when fused with Al_2O_3; curve (1) 30% Cr_2O_3 to 70% Al_2O_3; curve (2) calculated from Rankin and Merwin MgO–Al_2O_3 diagram; curve (3) 10% Cr_2O_3 to 90% Al_2O_3.

amount to measure, it was counted but not identified; (*d*) some samples contained small amounts of opaque material, and when this was sufficient in amount it was measured and counted. Opaque particles were not definitely identified but were believed to be either magnesium titanate or magnetite. That this method is practical is shown in such instances where crystal-phase compositions were approximately those contained in established constitution diagrams since they agreed closely in phase composition with the data calculated from the published phase-rule diagram.

Two series of fusions were made as follows: (1) A series in which 90% alumina and 10% chromium oxide was fused with variable amounts of other oxides and (2) a series in which the alumina-to-chromic oxide ratio was kept constant at 70% alumina to 30% chromium oxide. The results of the petrographic examination of the first series is recorded in Table I.

The data from Table I are incorporated in the graphs of Figs. 1, 2, 3, and 4. Figure 1 summarizes the chrome-corundum counts in which chromium oxide-alumina fusions with MgO additions from 0 to 5% were heated with SiO_2 from 0 to 3%. Figure 2 summarizes fusions similar to Fig. 1, but the treatment was made with titania (TiO_2); in Fig. 3, the treatment required FeO up to 5%. Figure 4 gives two curves, one of Cr_2O_3 10%, Al_2O_3 90% and another Cr_2O_3 30%, Al_2O_3 70%, to each of which MgO additions from 0 to 5% were made; these curves may be compared with the dashed-line curve, which is based on the Rankin and Merwin MgO–Al_2O_3 diagram.[2]

In all of the figures, the percentages of chrome-corundum that had been determined by the petrographic method described previously are plotted vertically.

III. Conclusions

(1) In an electric furnace fusion of MgO–Cr_2O_3–Al_2O_3 within the limits studied, silica up to 3% and to a lesser extent titania up to 3% tend to inhibit or decrease the solid solution of alumina in spinel (Figs. 1 and 2).

(2) As the amount of chromium oxide increases in a chrome ore-alumina fusion, the alumina becomes less souble in a $MgO(AlCr)_2O_3$ phase. The present experiments indicate this to be true up to a 30% replacement of Cr_2O_3 for Al_2O_3 (see Fig. 4).

(3) As the amount of iron is increased up to at least 5% FeO in a chrome ore-alumina fusion, the alumina becomes less soluble in the $(FeOMg)O$, $(CrAl)_2O_3$ phase (Fig. 3).

These conclusions of course are tentative, inasmuch as this study was made as part of a larger series of experiments having a practical purpose in the development of the fusion-cast chrome-alumina refractory; the compositions covered were limited in number and were selected primarily to fit in with basic experiments conducted in this laboratory.

RESEARCH LABORATORY
THE CARBORUNDUM COMPANY
NIAGARA FALLS, NEW YORK

GLASSHOUSE STONES*

By William L. Fabianic

Abstract

Most of the various types of glass stones actually found under operating conditions in furnaces melting soda-lime bottle glass are discussed. Each type is described in detail and photomicrographs of each kind of stone are shown. The possible source of each type of stone is considered along with general methods for its identification and elimination. Auxiliary aids to the petrographer, such as the use of solvent acids and chemical analyses, are mentioned. The stone specimens have been taken from flint, amber, and green-colored glasses.

I. Introduction

Many fine contributions have been devoted to the problem of glasshouse stones. The writings of Insley,[1] Thompson,[2] Wilson,[3] Peck,[4] Bowen,[5] Bellière,[6] and, more recently, the unusually splendid work of Holland and Preston[7] have dealt with the subject so thoroughly that further contributions are bound to duplicate some portions of their work. This repetition, however, is justified if the annual loss of glassware caused from stones can be decreased.

The present paper has aimed at the practical side with the thought of making it a guide to those having losses from stones.

Simple definitions of common glass factory phraseology are omitted as well as descriptions of general microscopic technique, Becke line, refractive index, and mineralogical data. Such information is amply covered by Larsen,[8] Winchell,[9] Johannsen,[10] and others.

---

* Presented at the Forty-Sixth Annual Meeting, The American Ceramic Society, Pittsburgh, Pa., April 5, 1944 (Refractories Division). Received May 13, 1944.

[1] (*a*) Herbert Insley, "Determination of Source and Means of Prevention of Stones in Glass," *Jour. Amer. Ceram. Soc.*, **12** [3] 132–52 (1929).

(*b*) Herbert Insley, "Study of Origin of Stones in Glass," *ibid.*, **6** [6] 706–16 (1923).

[2] C. L. Thompson, "Identification of Stones in Glass," abstracted in *Glass Ind.*, **17** [8] 265–68 (1936).

[3] G. V. Wilson, "Notes on Formation of Certain Rock-Forming Minerals in and about Glass Furnaces," *Jour. Soc. Glass Tech.*, **2**, 177–216 (1918).

[4] A. B. Peck, "New Glass Stone, $Na_2O \cdot 3CaO \cdot 6SiO_2$," *Jour. Amer. Ceram. Soc.*, **9** [6] 351–53 (1926).

[5] N. L. Bowen, "Identification of Stones in Glass," *ibid.*, **1** [9] 595–603 (1918).

[6] Marcel Bellière, "Crystallization of Pseudowollastonite by Devitrification of Glasses," *Glass Ind.*, **15** [8] 178–81 (1934); references to foreign journals in *Ceram. Abs.*, **13** [4] 84 (1934).

[7] A. J. Holland and Eric Preston, "Microscopical Examination and Identification of Crystalline Products in Commercial Glasses, I–II," *Jour. Soc. Glass Tech.*, **21** [87] 395–408 (1937); **22** [9] 82–98 (1938); *Ceram. Abs.*, **17** [9] 304 (1938); **18** [1] 17 (1939).

[8] E. S. Larsen, "Microscopic Determination of Nonopaque Minerals," *U. S. Geol. Surv. Bull.*, No. 679, 294 pp. (1921).

[9] A. N. Winchell, Elements of Optical Mineralogy, Parts I and II. John Wiley & Sons, Inc., New York, 1931.

[10] Albert Johannsen, Manual of Petrographic Methods. McGraw-Hill Book Co. Inc., New York, 1918.

II. Methods Used

(1) General Observation Procedure

(*A*) Select a representative number of the bottles or pieces of ware containing the stone. Using an ordinary glass cutter, deeply score an area, about 1 sq. in. in size, on the bottle side wall and having a stone in the center of it. Tap this specimen out of the bottle side wall by a sharp rap; continue this process until one or more stones have been taken from each piece of ware selected, as representative samples.

Check over this entire group of cut-out specimens and see if they can be divided into two groups, one containing stones which appear to be well rounded and partly in solution and the other containing new stones with sharp undissolved edges. If all have the same general appearance, there will naturally be only one original group, which may indicate roughly whether the stones have been present in the furnace a long or short time.

(*B*) Next, using a small hand glass, divide this group or groups into two classes, one class having all of the opaque-appearing stones and the other, the transparent or translucent types. The opaque stones generally, but not always, indicate refractory origin, and the translucent stones, either silica or devitrification products. With small clay stones, however, no conclusions can be drawn because they will also look translucent if they are partly in solution.

Devitrification stones can sometimes be detected by their irregular shape and translucent appearance. A bottle with a devitrification stone in it often breaks cleanly through the stone. A silica stone from unmelted sand or silica refractory often looks translucent, but in most cases the glass will fracture around and not through it.

In flint glass, silica drops sometimes give a bluish tint to the surrounding transition layer of glass. Refractory stones tend to tinge the adjacent glass a greenish or brownish color. Stones showing a streamer or tail attached to them indicate their source to be from above the glass level.

The foregoing observations, while very crude, can be made easily and quickly and sometimes result in a definite lead on the problem.

(2) Microsections

Regardless of whether any worth-while information is secured by the foregoing superficial examination, the

FIG. 1.—Source of stones in 100 lb. of flint cullet during heavy siege of stones.

next step is the preparation of suitable microsections. Several samples of each suspected type of stone must be prepared for microscopic examination. In some cases, especially for devitrification stones in flint glass, it is actually unnecessary to do any grinding down to a true thin section; the original piece of glass containing the stone can be used to identify the crystal. Some grinding, however, is usually necessary to prepare a section thin enough for identification purposes. If time permits, a genuine microsection should be made and mounted permanently in balsam. Microsections are necessary to identify opaque stones and also very fine devitrification crystals if they are thickly crystallized. Identification is made by studying the various properties of the stone.

It is often necessary, especially with silica stones, to break the stones out of the glass and to separate as many virgin particles of stone as possible with a pair of tweezers (a reading glass may be used if desired); the stones are then crushed in alcohol in an agate mortar, and the slides must be prepared with various oils to determine the actual index of the material. This process, of course, cannot be followed as long as the stone is embedded in the glass.

A partial chemical analysis can be secured for many of the stones. For stones suspected of being clay, this analysis contributes valuable information. The stones can be separated from the little squares of glass in which they are imbedded by heating over a Bunsen burner and drawing out into a thread with two pairs of tongs. The stones can be pinched out of the thread and a surprisingly clean specimen can be obtained. Owing to the presence of interstitial glass, the analysis of a stone that appears to be a solid mass of devitrified silica will never be very close to the theoretical composition

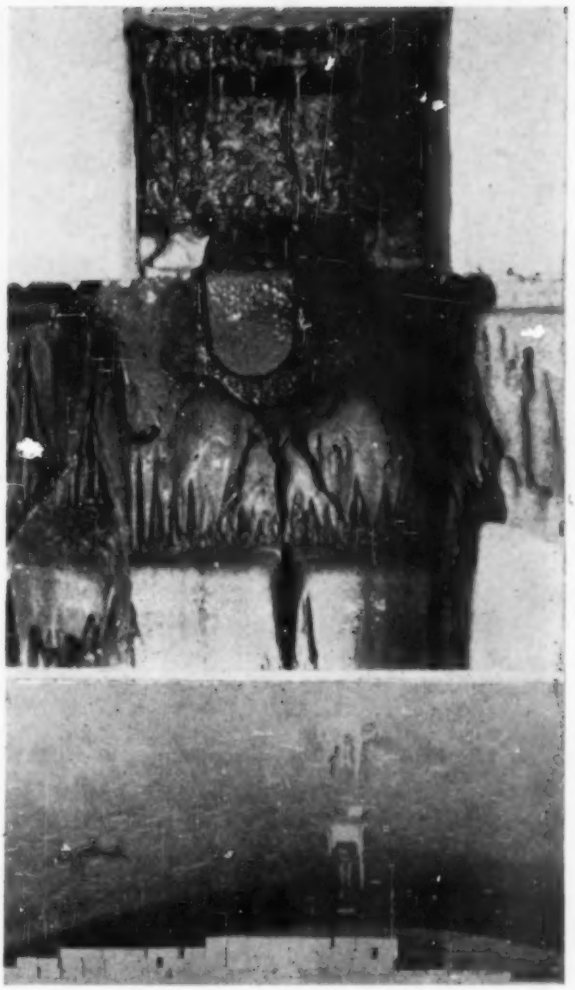

FIG. 2.—*Upper:* Refractory drips from refractory cover block over alcove of Owens revolving pot; *lower:* silica stalactites from around thermocouple block in furnace crown.

of the identified mineral. If the interpretation is correct, however, the analysis sometimes has an appreciable value, especially in the alumina content which is useful to verify the stones of clay origin.

Various additional tests are sometimes improvised, such as testing the solubility of soft, crumbly stones with dilute acids. Limestones and sulfates can be detected in this manner.

III. Source of Materials Examined

Nearly all of the specimens discussed in this paper are actual stones obtained from works practice and were the source of loss of ware. A few of them were taken from devitrification studies of glass in a laboratory crucible.

The complete and accurate history of the stones to be examined is most important in these studies because a simple identification of the stone will not decrease a continuing stone loss in the plant unless a specific and

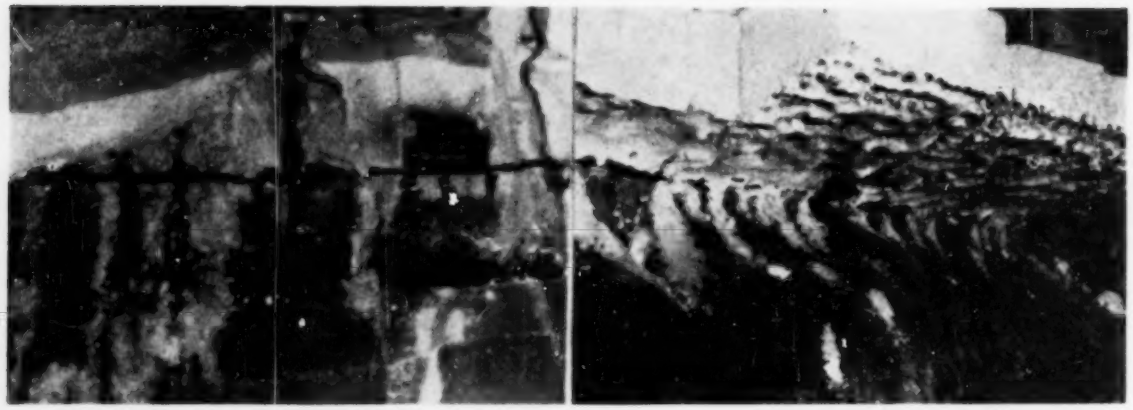

FIG. 3.—*Left:* Silica port sill melting and dripping down over top of flux block; *right:* shows how under side of silica sill block and tuck brick melts and drips down over flux block (prolific source of furnace slacks).

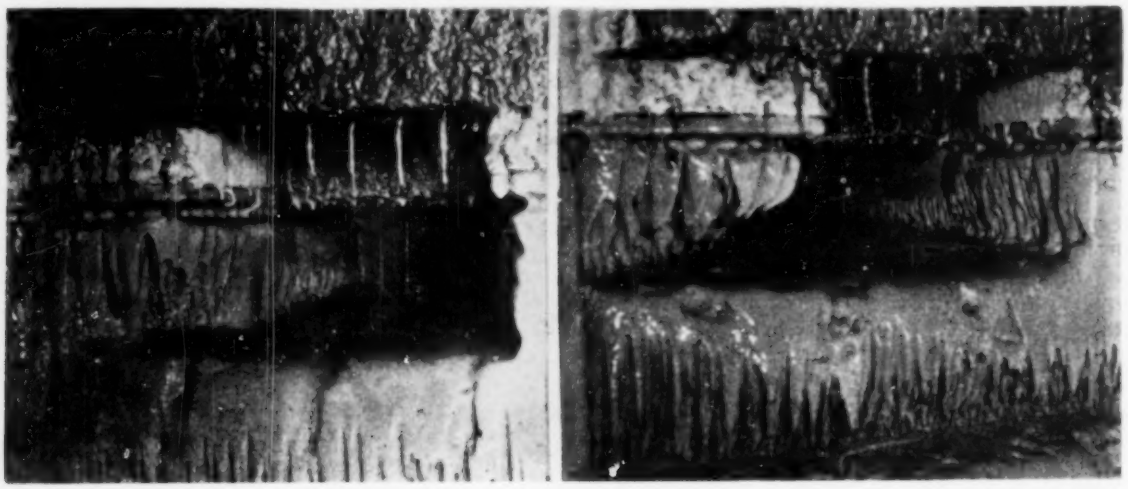

FIG. 4.—*Left* and *right:* Refractory block at entrance to forehearth slagging and dropping into glass; refractory slag also attacking silica supporting it and is obvious source of stones, slacks, and cords.

correct recommendation is made to eliminate the stone. This reasonable request for detailed information is sometimes impossible to obtain. A moment of reflection, however, should convince even the most hard-boiled supervisor that he will benefit by his cooperation because the history of the stone itself often indicates that certain changes have taken place that could affect the optical properties of the stone and thus would confuse its proper identification.

IV. Origin and Types of Stones

(1) Cullet

One prolific source of stones is contaminated factory-quarried cullet. Small chips or particles of refractory material become mixed with the cullet during furnace repairs when glass is being quarried from the furnace. This type of dirty cullet has been the source of severe stone losses. Pieces of such quarried cullet taken off next to the block with the transition layer adhering also cause stones. Particles from the porcelaneous transition layer can pass completely through the furnace and appear in the ware. Pieces of the refractory the size of a pinhead can and do cause trouble. The loss of ware due to stones mixed with quarried factory cullet is one source of loss that most factories have complete control over and can entirely eliminate by the selection or forking of the cullet.

The loss of ware due to stones in contaminated purchased or commercial cullet is sometimes a problem. Much commercial cullet is good clean washed material, but a lot of it contains cinders, pieces of brick, particles of concrete, and metals of various kinds. It is quite important for this reason to inspect purchased cullet closely.

Lehr cullet is generally innocent of causing stones unless it is that portion of the ware rejected initially for having stones as a defect. Large stones in lehr cullet can go through the furnace a second time, causing a recurrence of the same loss. Bottles containing large stones should not be included in the regular offware cullet.

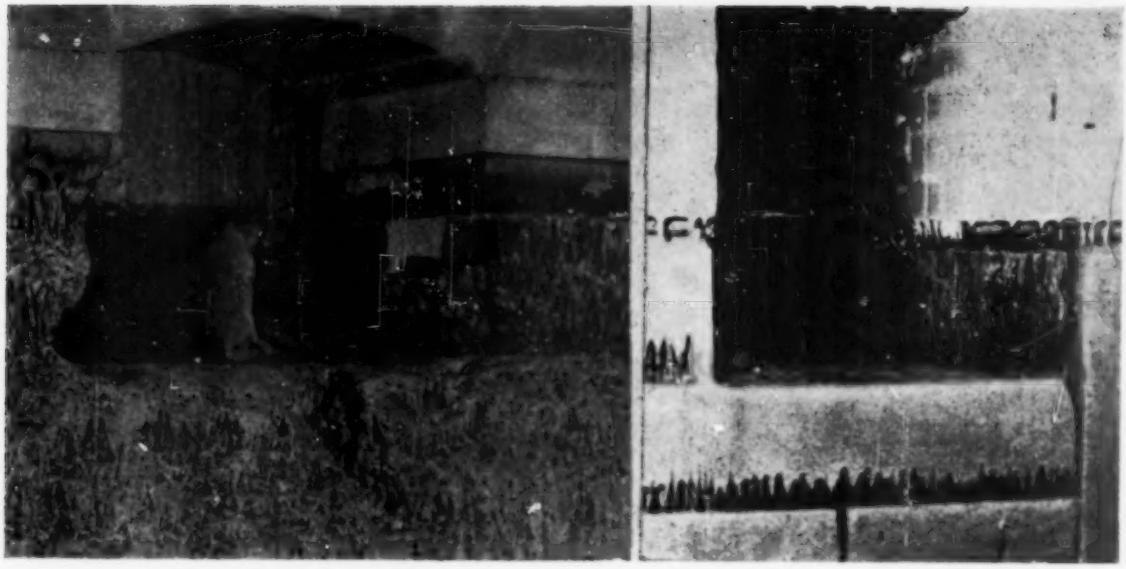

FIG. 5.—*Left:* Badly pitted and honeycombed flux block around entrance to feeder; *right:* bad flux block at corner of entrance to forehearth showing excessive wear with consequent stone emanation.

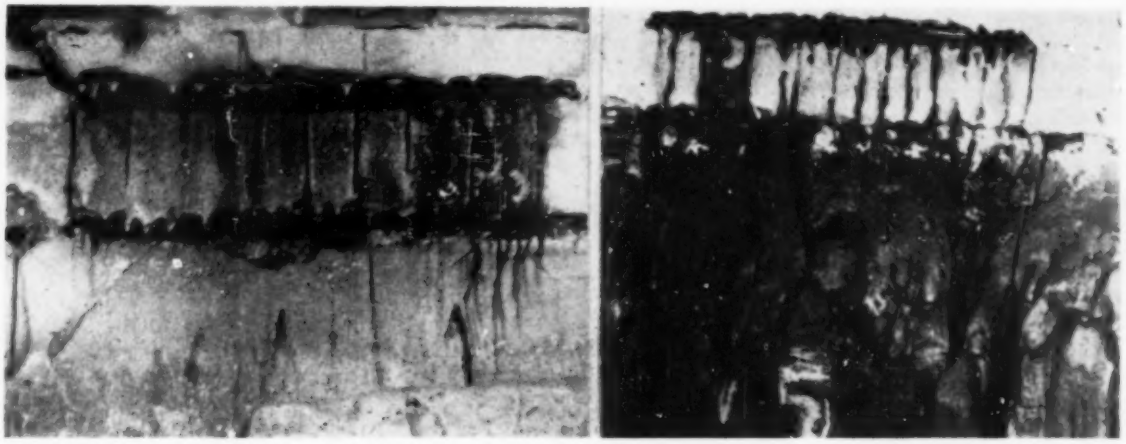

FIG. 6.—*Left:* Angle irons embedded into upper structure side wall, melting badly and running into furnace; *right:* showing how molten iron cuts away block below it; failure of refractories in front of these angles allows iron to be exposed.

Another much less frequent source of stone loss from cullet is caused by using too great a quantity that has formerly been decorated with ceramic colors. These fired colors, enamels, or glazes become reduced in going through the furnace and appear as metallic blobs or splotches on the ware.

If a siege of stones is encountered and they are suspected of coming from the cullet, a 100-lb. sample should be spread out on a clean floor and examined carefully and slowly.

If the offensive cullet has already been unloaded into a storage bin, it is pretty difficult to do anything about it. If, however, it is stored in an outside stockpile, such débris as pieces of refractory, cinders, and similar materials can be partly cleaned out by forking the cullet with a large, wide stable fork with tines a half inch apart. Washing the cullet with a fire hose also helps considerably.

Figure 1 shows a sample of stones found in a 100-lb. lot of flint cullet during a particularly heavy siege of stones. When the use of this cullet was discontinued, the stone loss ceased.

(2) Stones from Furnace Refractories

When all of the refractories used in furnace construction that are so located that they can contribute stones to the glass are considered, they obviously constitute a most prolific source of stones. They encompass all of the clay, silica, and special refractories used, both above and below the glass level, in such furnace parts

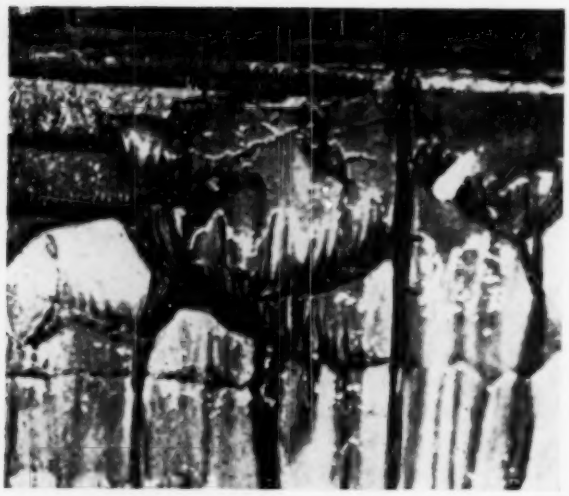

FIG. 7.—Flux block worn through at metal line and overcoated as possible source of stones.

as port jambs, port sills, port paving, port baffles, port snout side walls, furnace flux block, breast walls, end walls, mantle block, crown, bridge wall, tuck stones, runner block, all forehearth refractories, and Owens pot refractories, including the trough, plug, overhang block, pot, and jack arches. All cements and mortars used must also be included.

Sometimes fire-clay refractories are placed directly over and are supported by silica refractories. Their presence invariably results in a slagging action, particularly if they are located in the melter. The fire clay will slag a bit, forming a low-melting mixture with the silica, and the silica will be badly attacked. This attack can cause clay, silica, and nepheline stones, depending on how fast the action proceeds, on the temperature, and on the amount of batch dust present.

Figures 2 to 7 show a few possible sources of furnace refractory stones.

The elimination of stones of refractory origin in each case is a special problem and general recommendations are of little aid. If slag streams are entering the glass from the port openings, wind placed on the underside of the port sometimes helps to chill them. If the slag stream is caused by a baffle wall or shadow wall, the baffle can be replaced or the shadow wall can be dammed up. Stones from the metal line of the furnace can be decreased by maintaining a constant glass level, uniform temperature, and flame length in the furnace. Refiner stones can be generally aided by looking for local flame impingement of a burner and by lowering the temperature as much as possible.

It is general practice to lower the furnace temperature to decrease refractory stones, but if the stones are from the melter ports and are almost in solution, a slight increase in melter temperature sometimes will eliminate them. This procedure is naturally based on the fact that such an increase in temperature does not loosen new stones to a greater extent than it dissolves the old ones; the skill of the operator is also important in confining the temperature increase to the melter itself and not to the ports.

Refractory stones in the melter can usually be held to a low percentage by using a minimum of clay refractories, keeping fire clay away from silica, and operating the furnace with as little flame impingement and dust carry-over as possible. Refiners, forehearths, and revolving pots should be run at as low a temperature as possible and should avoid flame impingement, especially from oil. Naturally, the less batch dust that enters a furnace, the less slagging of refractories will take place.

(*A*) *Nepheline Stones:* Although nepheline stones ($Na_2O \cdot Al_2O_3 \cdot 2SiO_2$) could be discussed under clay stones (section (2) (*B*)) along with mullite and corundum, they will be listed separately to stress their importance.

Nepheline stones, streamers, or cords can be formed by the proper proportions of alumina, soda, and silica (sodium silicate) coming together under the conditions necessary to form nepheline as a transition layer on refractory surfaces.

Because any clay refractory subjected to the attack of soda-lime glass will acquire a transition layer composed of nepheline, corundum, mullite, and then virgin refractory, it is reasonable to find the presence of nepheline in many stones. Such stones can be formed either by the slagging of alumina-silicate refractories by batch dust or of silica refractories. When fire-clay and silica refractories slag in contact under the effect of alkali vapors, a combination of nepheline and clay stones can occur. If the source of formation is not too close to the working point, most of the solid particles that are included in the molten stream of refractory will be completely dissolved. The stream or cord of material, which was probably carnegieite above 2462°F., then emerges in the ware at lower temperatures, nearly all as nepheline. If the distance the stream or dripping has to travel is too short for complete solution and conversion to nepheline, the resultant stone will be a combination of nepheline and clay. The clay portion may be completely converted to mullite and some nepheline formed in cooling may be crystallized around it. If the original stone or size of the molten slag stream flowing into the glass is large enough to pull sizable pieces of refractory with it, corundum is also frequently present.

Such streams of material have originated and run out of the port openings, from breast walls down over the tucks, from burner block openings, the shadow wall fluxing down over the bridge-wall cover stones, mortar joints in forehearths, end-wall overhangs, and any local area abused by severe batch dust and flame impingement.

Nepheline can readily be recognized by its low double refraction, low index, and thick short prismatic crystals; it is in the hexagonal system.

Figure 8 shows a streamer or worm of material from flint glass that is converted almost completely to nepheline and a molten, high alumina-rich glass. A partial chemical analysis* of the stone shown in Fig. 8

* The writer is indebted to E. W. Summers, chief chemist, Owens-Illinois container plants, for all chemical analyses given in this paper.

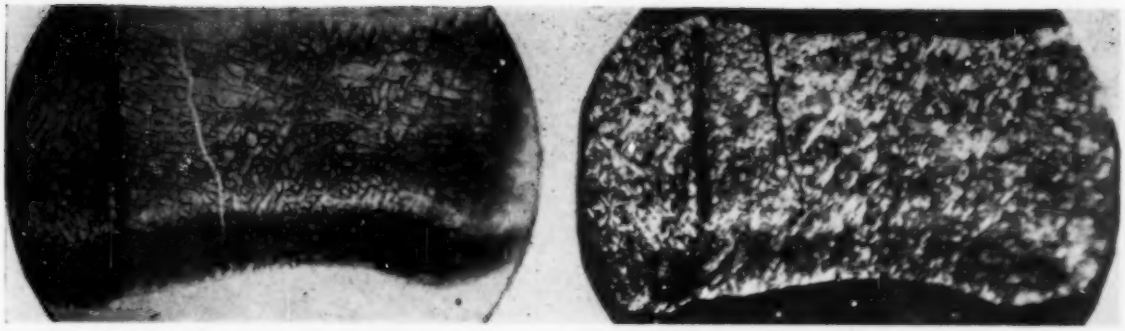

FIG. 8.—Flint glass; refractory streamer from port next to bridge wall with advanced nepheline development; *left*, transmitted light × 80; *right*, crossed Nicols × 80.

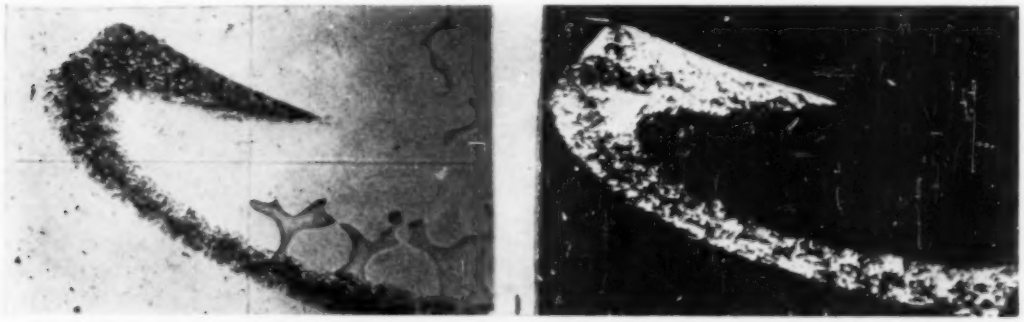

FIG. 9.—Flint glass; nepheline worm showing advanced crystallization; *left*, transmitted light × 80; *right*, crossed Nicols × 80.

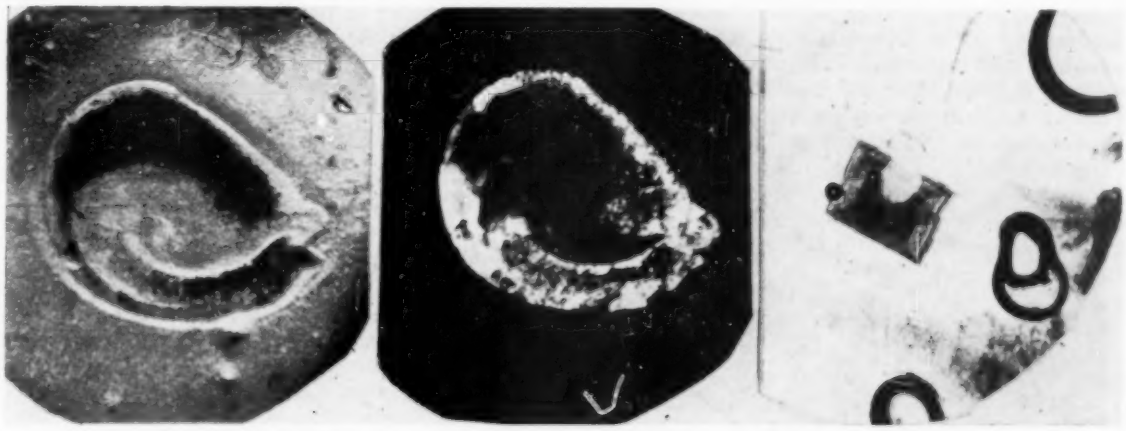

FIG. 10.—*Left* and *middle:* Amber glass; typical nepheline worm originating from clay bridge-wall cover block in melter; *left*, transmitted light × 80; *middle*, crossed Nicols × 80; *right:* cross section of nepheline crystal from clay crown drip composed almost entirely of nepheline, transmitted light × 125.

was found to be Na_2O 9.6, CaO 11.0, SiO_2 51.0, Al_2O_3 17.8, and BaO 1.33.

Figure 9 shows a nepheline worm that has been almost totally in solution and has crystallized chiefly as nepheline. A partial chemical analysis was SiO_2 62.04, CaO 12.03, MgO 7.28, Na_2O 7.60, and Al_2O_3 9.32.

Figure 10, *left* and *middle*, illustrates another typical nepheline worm found in the bridge-wall cover block. The stone analyzed SiO_2 52.00, Al_2O_3 28.00, Fe_2O_3 2.00, CaO 3.00, MgO 2.5, Na_2O 13.5, and TiO_2 trace.

(*B*) *Clay Stones:* A discussion of clay stones (mullite, $3Al_2O_3 \cdot 2SiO_2$, and corundum, Al_2O_3) naturally overlaps that of nepheline stones because they are generally inseparable associates.

Insley,[1] Peck,[4] Bowen,[5] Thompson,[2] and others have given a complete description of refractory stones from

FIG. 11.—Flint glass; clay stone almost completely altered to mullite and corundum, transmitted light × 225.

have pronounced borders of long mullite needles growing around them.

A partial chemical analysis of the stones shown in Fig. 12 is given as well as the analysis of the glass immediately surrounding the stones.

	Stones (%)	Adjacent glass (%)
SiO_2	69.74	72.39
Al_2O_3	6.29	1.95
CaO	6.88	8.67
B_2O_3 } Na_2O }	17.09	16.10

Corundum stones, common associates of mullite stones, are one of the resultant products from solution and conversion of clay refractories to mullite, corundum, and nepheline. The most characteristic appearance of corundum is in the form of thin, hexagonal

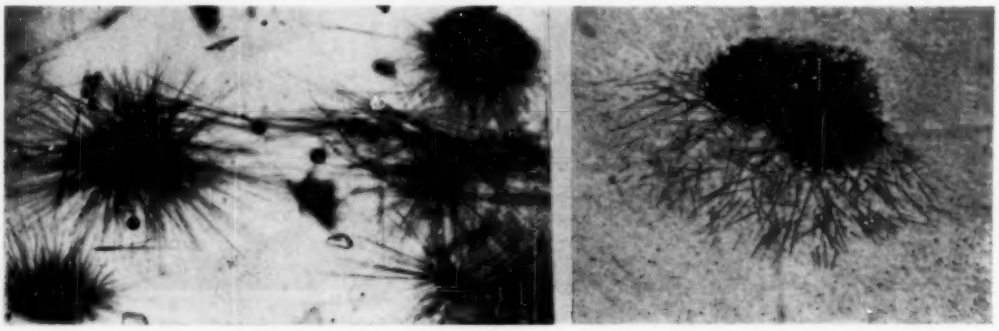

FIG. 12.—*Left* and *right:* Mullite growth around clay particles below flint glass line, transmitted light × 100.

above and below the glass line and from the hotter and cooler portions of the furnace. The author agrees in general with such deductions as (1) the source of large corundum crystals is above the glass line and (2) stones not far advanced in solution are from the cooler portions of the furnace, and other basic facts. The writer, however, has also found that it is not an easy matter in a majority of cases to determine definitely whether the stones were from above or below the glass line and has found in some cases that stones were being contributed within an inch of each other both below and above the glass level at the same time as the block were cut back at the metal line. This is probably due in part to the almost revolutionary use of special refractories in present-day container furnaces.

Mullite, which is identified by its index of refraction, birefringence, extinction, and elongation, crystallizes in groups, spherules, fans, or brush-heap structure. Its presence generally indicates the source as an alumina-silica refractory except in rare cases where it originates from minerals found in the raw batch materials. Mullite crystals derived from molten cast material generally exhibit the property of pleochroism.

Figure 11 shows a clay stone taken from below the glass level of a flint furnace almost completely altered to mullite and corundum. This type of stone indicates that the clay particle was exposed to the glass for a long time.

Figure 12 shows stones from grog in a flux block that

plates. From below the glass level, these plates can be extremely small; above the glass level, they are often quite large. Their colorless nature and their hexagonal form generally identify them; if turned up on edge, they can be detected by their very high index of refraction, low birefringence, and positive elongation.

A stone composed wholly of corundum plates indicates that it has been in the glass long enough for all accompanying associated minerals to go completely into solution, the corundum remaining due to its extremely refractory nature.

Figure 13 shows a stone in an advanced stage of solution from a molten cast refractory. It is composed of large well-developed mullite crystals, plates of corundum, and an alumina-rich glass plus incipient nepheline. This stone was taken from a flint furnace.

Figure 14, *left*, shows a large crystal of alpha-corundum, which in addition to having the characteristic hexagonal plate form also shows sets of parallel lines that are in the direction of the principal axes. This structure coincides superficially with the illustration mentioned by Holland and Preston* on the Widmanstätten structure. Reference to the works of Sauveur[11]

* See Holland and Preston, p. 407 of footnote 7.

[11] Albert Sauveur, Metallography and Heat-Treatment of Iron and Steel, p. 212, 2d ed. Publ. by Sauveur and Boylston, Cambridge, Mass., 1920. 486 pp.

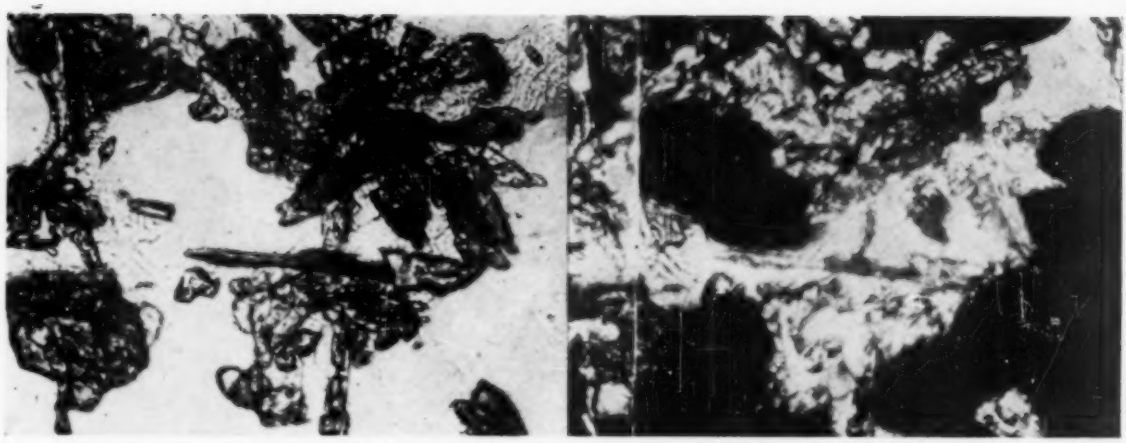

FIG. 13.—Stone in advanced stage of solution from molten cast refractory; *left*, transmitted light × 80; *right*, crossed Nicols × 80.

FIG. 14.—All flint glass samples; *left:* large corundum crystal with characteristic hexagonal plates, transmitted light × 125; *middle:* clay stone composed of corundum and mullite, indicating advanced solution of stone, transmitted light × 80; *right:* stone composed entirely of plates of hexagonal corundum; complete solution of nephelite and mullite indicates stone was in glass a long time, transmitted light × 80.

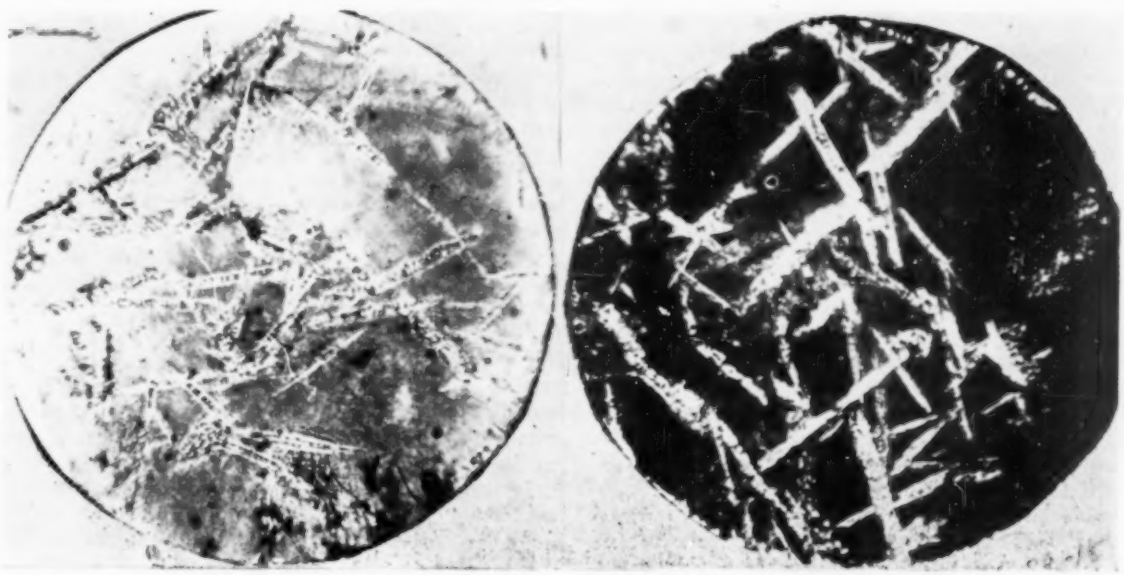

FIG. 15.—Advanced conversion of silica crown drop to large crystals of tridymite; *left*, transmitted light × 80; *right*, crossed Nicols × 80.

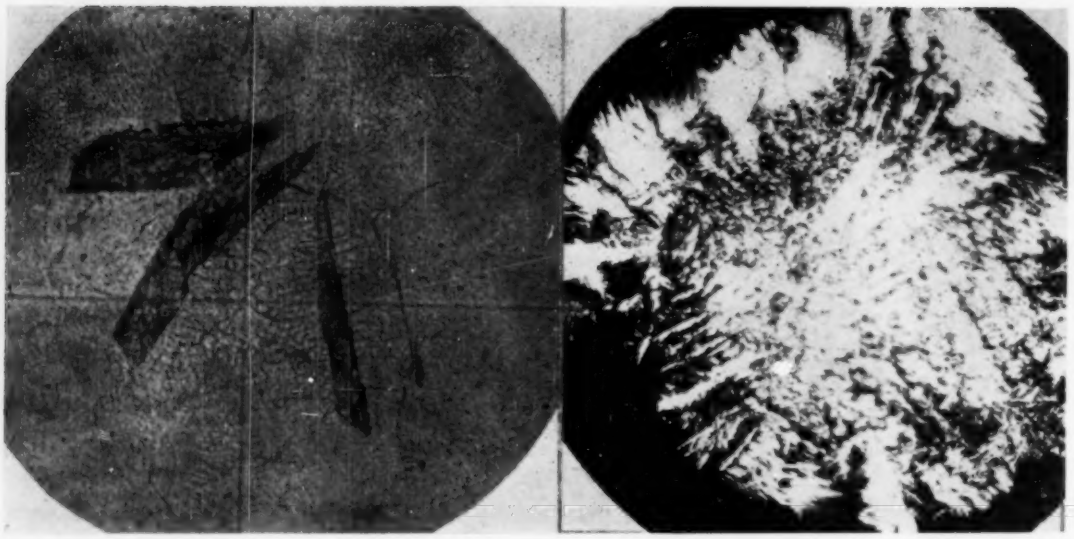

FIG. 16.—Spall from silica refractory going into solution; abundant wedge-shaped tridymite; *left*, transmitted light × 125; *right*, crossed Nicols × 125.

indicates this relationship to be so remote as to be of little consequence. Figure 14, *middle* and *right*, illustrates two more clay stones that have reached an advanced state of solution as shown by the high percentage of mullite and corundum present.

(*C*) *Silica Refractory Stones:* These stones are generally traceable to spalls or drips from the silica refractories some place in the furnace. A piece of silica brick may show original quartz grains plus tridymite and will not look a whole lot unlike a section of the refractory itself. The tridymite will be present as a result of conversion from quartz, which generally means wedge-shaped twins. A quartz grain, however, from unmelted sand or other highly siliceous refractory may have the same wedge-shaped twins. A silica dropping from the under side of the crown might be completely converted to large crystals of tridymite.

Figure 15 shows large tridymite crystals in the extreme lower tip of a crown dropping from a silica stalactite. Figure 16 shows a piece of silica spall almost in solution. The analysis of the silica stone in Fig. 15 was as follows: SiO_2 89.3, Fe_2O_3 and Al_2O_3 2.31, CaO 3.29, MgO 0.18, and Na_2O 4.41.

(*D*) *Special Refractory Stones:* Owing to the increasing use of zirconium refractories and cements as standard materials in many glass furnaces, there is the possibility of encountering occasionally some zirconium stones. The author has not been able to identify such stones definitely as to their exact mineral character and will simply refer to them as zirconium stones rather than the oxide (ZrO_2) or silicate ($ZrSiO_4$). Their index is so high as to be undeterminable; they have strong birefringence colors and good double refraction; they resemble an evenly elliptical oval and most of them are 0.028 mm. and under in size. If the operator can obtain a uniaxial positive interference figure on this type of stone, it would indicate zircon and would eliminate baddeleyite. Once zirconium stones are identified as such, the operator will never again have much trouble in recognizing them because of their high index and characteristic colors.

(3) Batch Stones

Only a few materials from the batch that sometimes do not entirely go into solution will be discussed under this heading. These materials include grains of unmelted sand, andalusite, feldspar, and lime. The silica crystallization from accumulated scum at the bridge wall or at dead corners of the furnace could be included under this heading, but it will be omitted here and will be covered under the discussion of devitrification stones in section IV (4).

In general, the best way to avoid batch stones is to use fine-grained raw materials. They should go into solution under conditions imposed by the maximum rate of pull intended for the furnace. It is particularly important to guard against coarse-grained sand.

The sand should also be free of all refractory minerals, clays, or clusters of grains. It is rarely necessary to worry much about anything but the sand, although reasonable precautions should be taken with the feldspar, soda, lime, and other materials. Stones are sometimes caused by coarse-grained coloring materials used in the manufacture of amber and green glasses, but this source is one that a plant can detect almost at once.

Figures 17 and 18 show the familiar example of unmelted sand grains; the sample shown in Fig. 17 was taken from scum in a cool corner of a flint furnace. Figure 18 shows sand grains from the batch that indicate practically no solution; owing to their lack of solution, their source was found to be between the refiner and orifice opening as was suspected.

Figure 19 shows a batch stone that is rather rare but which actually can occur under certain conditions. The feldspar ($Na_2O \cdot Al_2O_3 \cdot 6SiO_2$) causing this stone was quite coarse and damp, permitting almost unal-

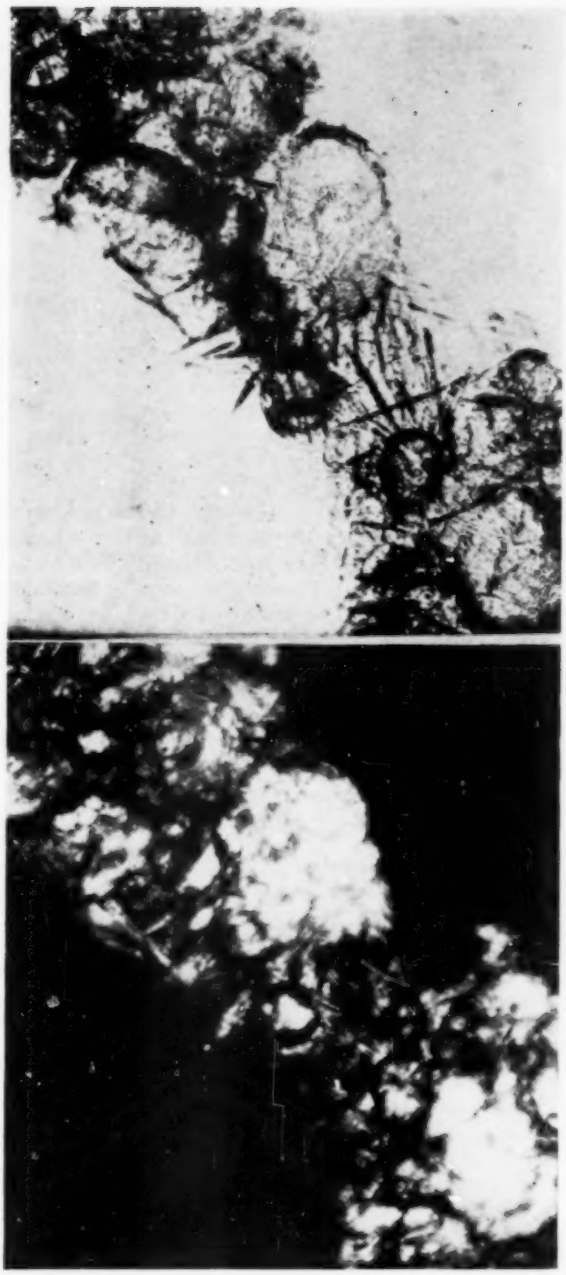

FIG. 17.—Flint glass; quartz grains from batch partly in solution and surrounded by wedge-shaped tridymite crystals; *upper*, transmitted light × 80; *lower*, crossed Nicols × 80.

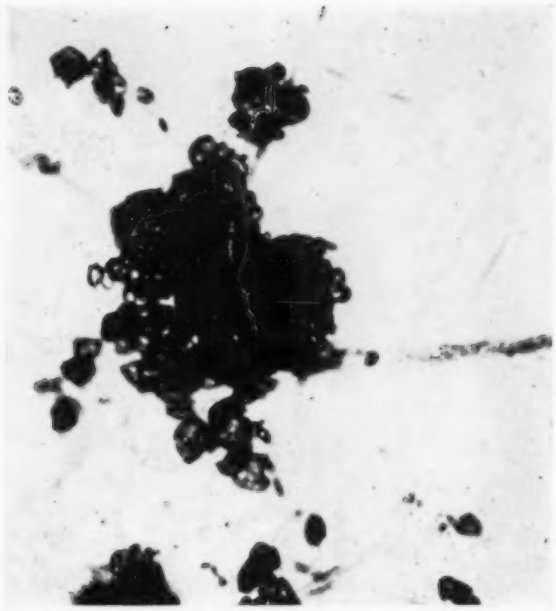

FIG. 18.—Unaltered sand grains from flint glass batch; transmitted light × 32.

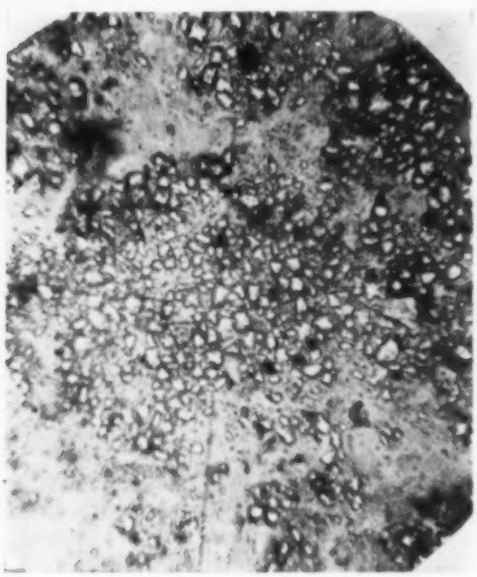

FIG. 19.—Amber glass containing feldspar stone caused by coarse-grained feldspar and balling of material; not a commonly occurring stone; transmitted light × 80.

tered feldspar grains to pass completely through the furnace.

Figure 20 shows a stone that was the cause of a considerable loss of ware before it was traced to its source and eliminated. This loss was caused by the appearance of small white stones in the ware. An examination proved these stones to be grains of andalusite ($Al_2O_3 \cdot SiO_2$) about 0.4 mm. long. The stone itself consisted of a single grain or crystal bordered by a rim of nepheline. These stones are a good illustration of the property sometimes exhibited by sillimanite, kyanite, and andalusite in the presence of an active flux and under conversion temperatures of almost direct conversion to nepheline with but a small amount of intermediate mullite. The andalusite can be distinguished from mullite because it is biaxial negative and mullite

FIG. 20.—All flint glass; *left* and *middle:* andalusite grain with unaltered core and fringe of nepheline around border; *right,* andalusite stone with unaltered core and fringe of nepheline around border; *left* and *right:* transmitted light × 80; *middle,* crossed Nicols × 80.

is biaxial positive; both have parallel extinction to longitudinal sections and symmetrical extinction in cross sections.

Andalusite is distinguished from sillimanite by its weaker birefringence, optical character, and lower index. Kyanite is distinguished from andalusite, sillimanite, and mullite by its extinction angle of 30 degrees and its higher index. The source of these stones was found to be the sand used in the batch and was immediately eliminated by changing sands.

This particular discussion concerns andalusi e, but the author has experienced exactly the same condition in which kyanite grains in the sand are the offender instead of andalusite. Any other refractory mineral would naturally be a similar source of loss.

Another actual cause of a severe stone loss was large balls of compact limonite, which appeared in the ware in a partially unmelted condition under a heavy load. It was discovered that these stones were being dredged out of the lake along with the sand used in the batch.

A loss from stones $^1/_4$ in. in diameter was caused by large clusters or lumps of wet lime. They appeared in the ware and were only slightly covered with a thin film of glass. When the glass was cracked off and a few cubic centimeters of hydrochloric acid was poured upon them, they fizzed up and almost completely disappeared, evolving CO_2 gas. These lumps of lime had actually passed through the furnace and had retained enough CO_2 to give a violent reaction with acid. An analysis of one of the large stones was as follows: CaO 70.65, SiO_2 21.83, R_2O_3 0.78, and ignition loss 0.00%.

(4) Devitrification Stones

Devitrification stones in bottle glass are a source of continued annoyance even though their cause and origin are fairly well understood. An improper liquidus point, which is influenced by temperature gradient, batch inhomogeneities, incorrect glass composition, viscosity of the glass and rate of cooling, reheating of the glass, surface volatilization, incorrect furnace design, and other causes, contributes to the formation of devitrification stones. The vexing problem of devitrification is especially associated with colored glasses due, in part, to their poorer transmission of light and heat. These stones may be distinctly crystalline and of fairly large size or in such a fine state of subdivision as to appear milky or opal. The external form of some devitrification products as a method of identification may be very misleading because of the various crystal forms some of them may assume.

The actual process of devitrification is a fascinating study and has been thoroughly covered by Morey.[12] He describes completely by test and by equilibrium diagrams the mechanics of the formation of devitrite, wollastonite, diopside, tridymite, cristobalite, and quartz. Liquidus temperatures and primary phases are shown with various eutectics and the simultaneous crystallization of two compounds. A study of this work makes clear how tridymite and devitrite, wollastonite and devitrite, or other related compounds may occur together. It also shows that cristobalite sometimes occurs when tridymite is expected and vice versa. This discussion explains why the usual primary phase of devitrite in commercial soda-lime bottle glasses is often absent and beta-wollastonite is found in its place. The complexities of all of the various types of devitrification are well defined, and Morey also shows how easily devitrification can be upset by outside influences of inhomogeneities in the glass and batch.

Silverman[13] has contributed valuable information on the effect of certain ingredients in a glass composition on the position of certain line boundaries.

In the elimination of a siege of devitrification stones, each individual case becomes a special problem. The composition and viscosity of the glass in question are assumed to be such that the liquidus point is within working range of the operating conditions.

---

[12] G. W. Morey, Properties of Glass, pp. 35–74. Amer. Chem. Monograph Series, Reinhold Publishing Corp., New York, N. Y., 1938. 561 pp.; *Ceram. Abs.*, **18** [2] 48–49 (1939).

[13] (*a*) W. B. Silverman, "Effect of Alumina on Devitrification of Soda-Lime-Silica Glasses," *Jour. Amer. Ceram. Soc.*, **22** [11] 378–84 (1939).

(*b*) W. B. Silverman, "Effect of Alumina on Devitrification of Sodium Oxide-Dolomite Lime-Silica Glasses," *ibid.*, **23** [9] 274–81 (1940).

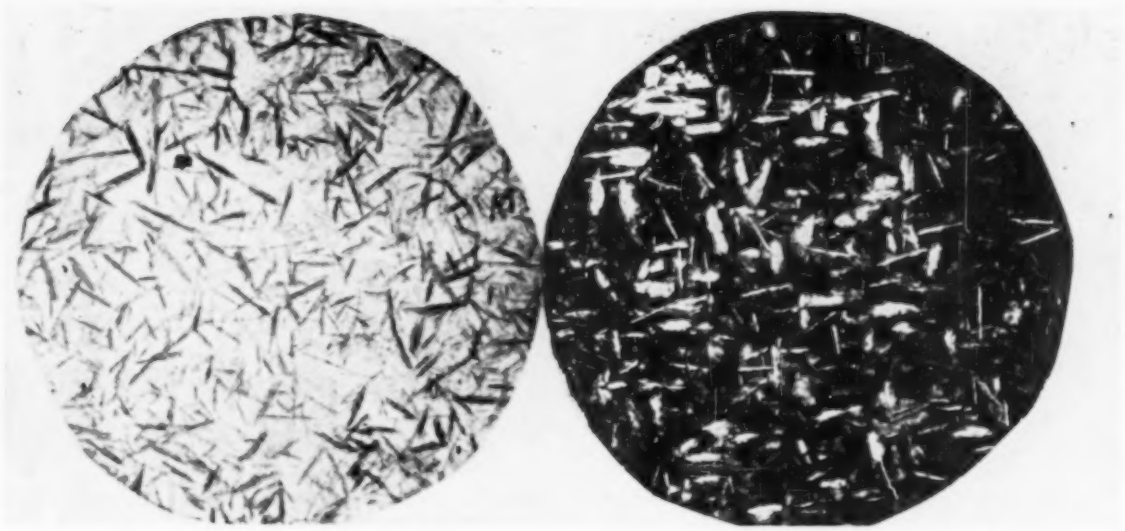

FIG. 21.—Flint glass; solid mass of hexagonal plates of tridymite turned on edge; *left*, transmitted light × 100; *right*, crossed Nicols × 100.

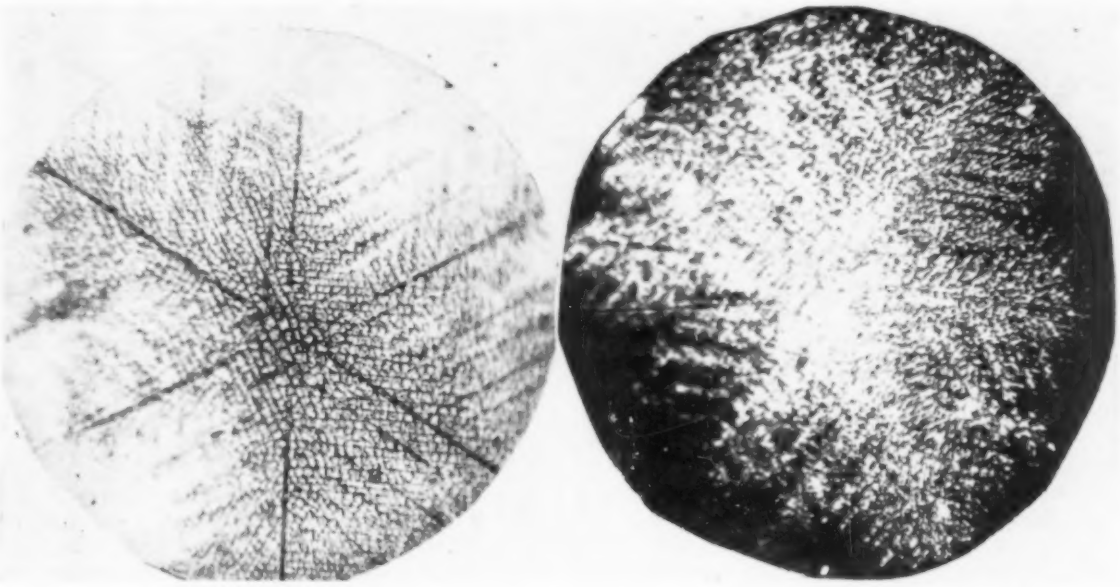

FIG. 22.—Flint glass with hexagonal plate of tridymite showing continuation of three half axes and underdeveloped main axis; *left*, transmitted light × 225; *right*, crossed Nicols, × 225.

If these stones appear in flint glass, a temperature survey of the complete furnace should be taken as quickly as possible, including pots, alcoves, corners, and forehearths. If the liquidus temperature of the glass is known, the operator can judge whether any portions of the furnace are cool enough to allow devitrification to proceed. He should then know whether the glass has been allowed to remain stagnant long enough or has had a slow enough movement from that area to permit time for devitrification. If the trouble occurs in colored glass, the temperature check, although still important, can be relegated to second place and a load change on the furnace should be sought. The furnaces melting colored glass will often have thick masses of devitrified glass on their bottoms and in the colder corners of the melter, refiner, and alcoves. A load change disturbs and changes the convection currents along the bottom and side walls and pulls particles of devitrification away from these masses. A change in load disturbs the convection currents in flint furnaces, but it rarely raises or disturbs actual devitrification products. In either case, raising the temperature at the suspected location or establishing a uniform load will generally clear up the trouble.

(1944)

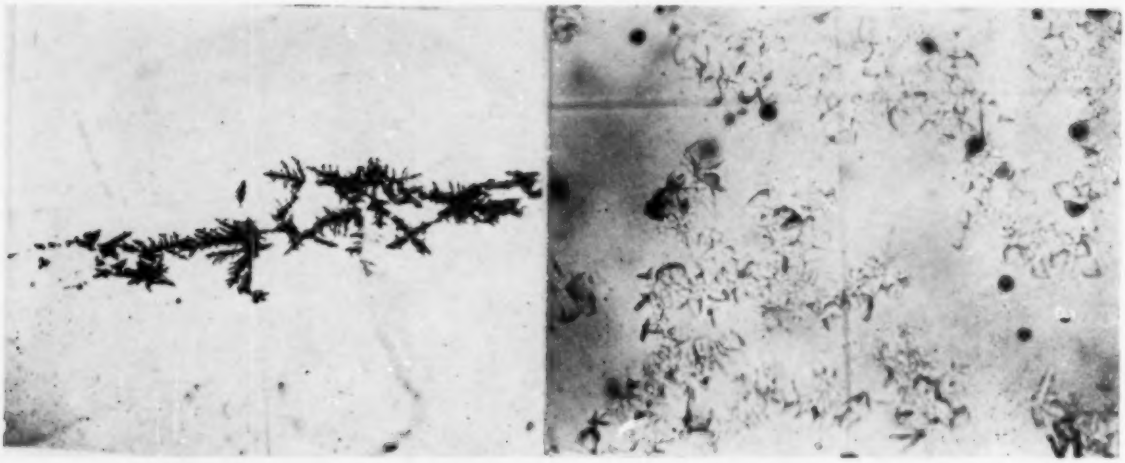

FIG. 23.—Amber glass samples; *left:* string of tridymite crystals in silica-rich cord of bottle glass, transmitted light × 100; *right:* crystallization of tridymite plates, transmitted light × 100.

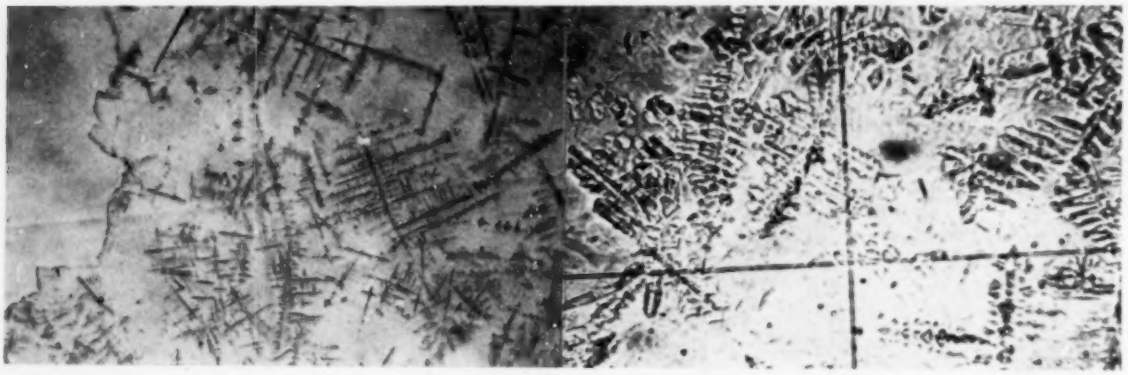

FIG. 24.—Flint glass showing typical crystals of tetrahedral cristobalite being pulled or floating out into glass stream; *left,* transmitted light × 80; *right,* transmitted light × 225.

If devitrification stones appear after a shutdown, they are generally caused by a local temperature condition in the refiner or forehearths and devitrification will disappear within a short time after the temperature is brought up to operating conditions.

If a furnace is fairly old and has water patches on it, a mass of devitrified glass may be formed on the inside surface and may be pulled off into the glass. This condition can usually be corrected unless it occurs because of a waterbox on the throat when the correction is more difficult.

A more unusual, but by no means rare, cause of devitrification stones is the presence of inhomogeneities in the batch resulting from large coarse-grained sand or limestone. An error in weighing the batch caused by inaccurate scales or by excessive moisture in some shipment of material will often cause temporary periods of devitrification.

Devitrification stones in colored glasses are sometimes impossible to avoid owing to improper furnace design. Furnaces for colored glasses should be designed to eliminate as many dead corners as possible and also to allow a minimum of dead glass to form on the bottom, where it is disturbed by load changes and convection currents.

Any device that will aid in introducing homogeneous glass to the furnace or that will homogenize the glass after it is introduced to the furnace will naturally help to decrease the presence of devitrification stones.

Chronic doses of forehearth devitrification sometimes indicate that, under the operating conditions employed, the glass is cool enough along the bottom and sides to form patches of devitrification. Additional insulation generally corrects this condition.

Although it is usually safe to raise the melter temperature of a furnace slightly when devitrification stones persist, if refractory stones are also present some care must be exercised or the increased temperature may loosen more refractory material. Thus when the devitrification stones are eliminated, they will be replaced by refractory stones.

(*A*) *Quartz:* Quartz (SiO_2) generally appears as a glass stone when it is derived from silica refractory or unmelted sand grains in the batch. Both of these sources have been discussed previously in this paper. It can occur as a devitrification product under certain

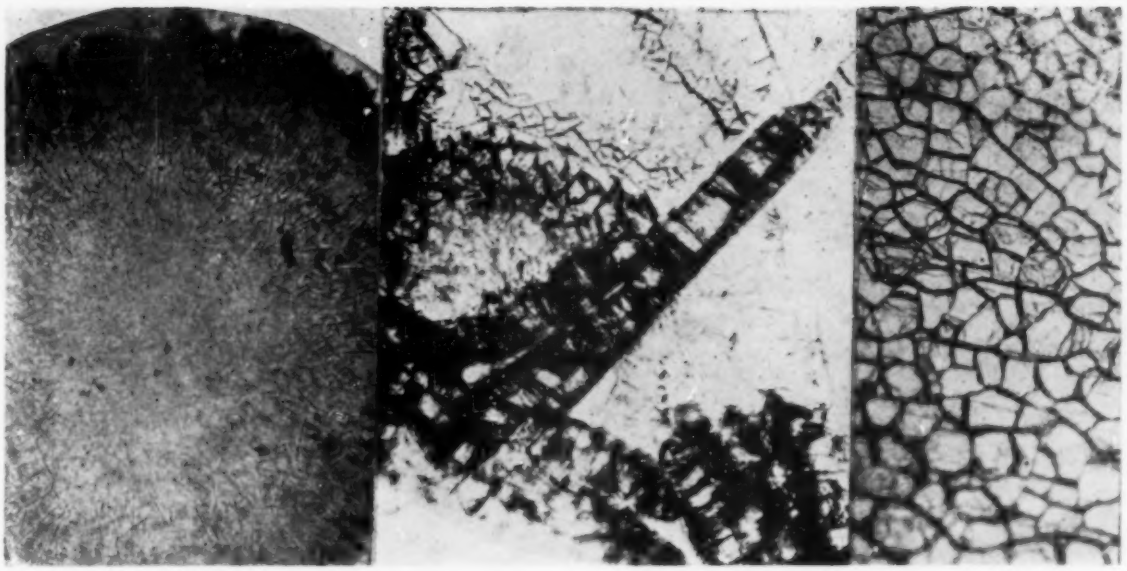

FIG. 25.—*Left:* Flint glass showing spherulite of cristobalite which usually characterizes slow cooling, transmitted light × 100; *middle:* amber glass showing large massive tridymite crystals and patches of cristobalite, transmitted light × 80; *right:* amber glass showing cristobalite in scum, transmitted light × 225.

unusual conditions, but these are so rare that the occurrence of quartz as a devitrification stone will not be discussed here. Quartz grains from coarse sand or resulting from batch separation accumulate in the dead corners of the furnace and form patches of silica scum and siliceous glass. The partial solution of these grains can result in the crystallization of many and varied forms of cristobalite and tridymite. Any of the forms of silica may crystallize owing to the presence of various fluxes so that a complete departure from strict phase-rule behavior is frequently encountered.

Quartz, which is hexagonal, is recognized by its well-rounded grain shape, weak birefringence, and index of refraction; it is uniaxial positive in optical character. Figure 17 shows quartz grains partly in solution that were accumulated in undissolved scum in a cool corner of a flint furnace.

(*B*) *Tridymite and Cristobalite:* Tridymite (SiO_2), under ideal conditions, is stable between 1598° and 2678°F. These stability relationships, however, are not sharply defined in the presence of fluxes so that tridymite may turn up in unexpected places. The same is true of cristobalite (SiO_2), which is supposed to be stable above 2678°F.

Tridymite is found in the scum on glass surfaces, in batch stones, and as a straight devitrification product from the glass. It also occurs in crown drops, generally as large wedge-shaped crystals. In scum, tridymite occurs both as hexagonal plates and wedge-shaped twins. Anhedral tridymite is also frequently encountered.

Tridymite can be recognized by its index, negative elongation, and optical character, which is positive. Its crystal form of wedge-shaped twins, its hexagonal plates generally turned on edge giving a lathlike or needle appearance, and its anhedral form also greatly aid in its identification. It has a rather low birefringence in glass. At glassmaking temperatures, tridymite belongs to the hexagonal group, but under 242.6°F., it is orthorhombic.

Cristobalite occurs frequently when quartz is converting to tridymite. In the majority of cases, the author has found cristobalite occurring as skeleton crystals. It is invariably an associate of tridymite in silica-scum formations and batch stones and can also devitrify directly from the glass. It can be recognized by its very low double refraction, index, and distinctive tetrahedral crystallization and parallel growths. The termination of most of the characteristic cristobalite dendrites is a small octahedron. The main axes of the tetrahedral structure are at right angles to each other. Hexagonal skeleton crystals of cristobalite may occur and, when crystallizing in this manner, the axes are sometimes trigonal; in other words, they do not extend on through the central axis as they generally do in the case of hexagonal tridymite.

All types of silica devitrification may occur as spherules, solid masses, or scattered through the glass.

Figure 21 shows tridymite taken from a thick heavy scum in a dead corner of a flint glass furnace.

Figure 22 shows a hexagonal crystal of tridymite taken from large white flakes appearing in the finished bottles from a flint furnace.

Figure 23, *left*, shows a string of tridymite crystals separating out as a result of inhomogeneous glass along a silica-rich cord in amber glass; Fig. 23, *right*, shows a thickly crystallized area of tridymite. These are all tridymite plates; the writer suspects that they are anhedral, but the section was not good enough to verify this.

Figure 24, *left*, shows the same stone at low magnification; Fig. 24, *right*, shows high magnification; it also brings out the dendritic structure and in a few instances

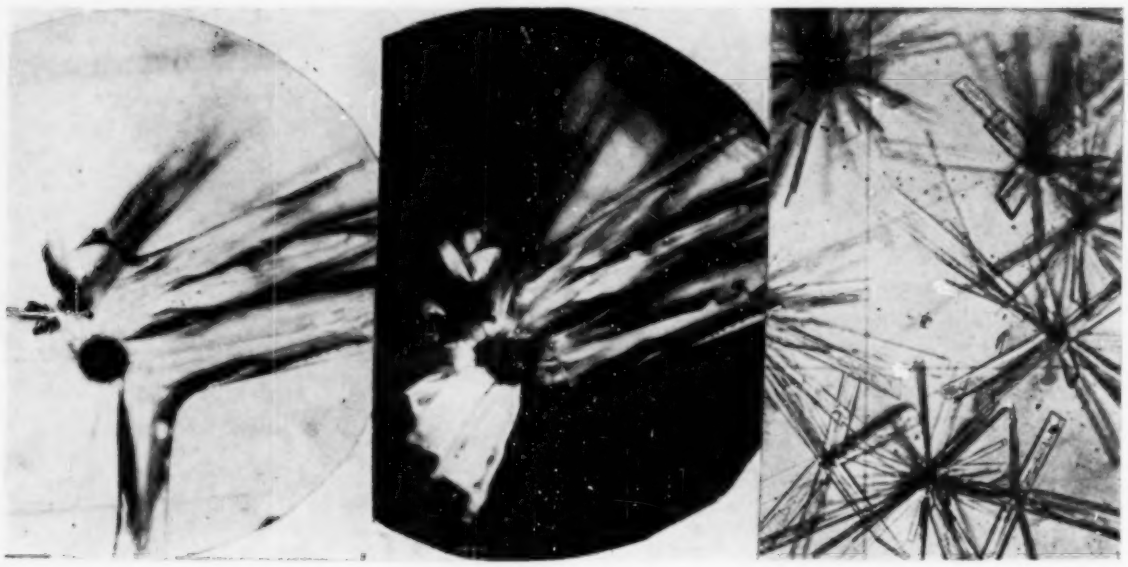

FIG. 26.—*Left* and *middle:* Amber glass sample from side wall of bottle showing large crystals of wollastonite forming around seed in glass as nucleus; *left*, transmitted light × 80; *middle*, crossed Nicols × 80; *right*, green glass sample from bottle side wall showing typical growth of wollastonite crystals, transmitted light, × 80.

shows clearly how the spearheads of cristobalite tend to terminate in an octahedral shape.

Figure 25, *left*, shows a cross section of a pure white ball or spherulite of silica; an analysis of the almost solid material making up this stone was SiO_2 73.5, CaO 5.70, MgO 4.18, Na_2O 16.92, and TiO_2 0.058. Figure 25, *middle*, shows a mixture of very large and well-developed tridymite and some patches of cristobalite. This sample represents white scum at the bridge wall over the throat of the amber furnace. Figure 25, *right*, is a magnified section of one of the patches of cristobalite shown in the middle cross section. A partial analysis of a solid portion of this scum was SiO_2 81.14, Na_2O 11.23, and CaO 6.89.

(*C*) *Wollastonite* ($CaO \cdot SiO_2$): Beta-wollastonite is one of the most familiar devitrification stones encountered by the glassmaker. It is the material to which the well-known expression "dog" has been applied. Wollastonite stones may emanate from solidified glass in the bottom or cooler portions of the furnace, from the decomposition of devitrite, or from the clear glass itself. If it appears as spherulites, it has probably cooled and formed fairly fast. The familiar lath-shaped crystals indicate slower cooling and formation. The crystals may occur as fan growths, parallel growths, spherulites, and in rare cases as prisms. Under proper conditions, wollastonite crystals sometimes attain extremely large size. The author has samples of wollastonite spherulites more than $1\frac{1}{2}$ in. in diameter that were taken from the nose end of a furnace after cooling down.

Wollastonite can be recognized by (*a*) the index of refraction, (*b*) parallel extinction, which it shows because its elongation is usually parallel to its b-axis, (*c*) biaxial negative optical character, and (*d*) shape of crystals. It is monoclinic and the elongation is generally positive. A careful observation and study will easily enable crystals of wollastonite to be discerned from mullite because they are inherently different, generally being wider.

Wollastonite can be distinguished from tridymite by its index and from diopside by its parallel extinction. A study of that part of the ternary system, Na_2O–CaO–SiO_2,[14] will show that beta-wollastonite and devitrite ($Na_2O \cdot 3CaO \cdot 6SiO_2$) are often associated as primary and secondary phases, the devitrite sometimes breaking down around 1922°F. and forming wollastonite. This phenomenon is illustrated very nicely by Silverman.*

Pseudowollastonite is the high-temperature form of wollastonite that is stable at temperatures above 2174°F. It is hexagonal, and its main associate appears to be cristobalite. Pseudowollastonite or alpha-wollastonite, which has been described in detail by Bellière,† can be distinguished from tridymite plates by its higher index.

Figure 26, *left* and *middle*, shows a cluster of well-formed ribbon or lathlike wollastonite crystals that have crystallized around a small seed in amber glass as a nucleus. The large crystal at the extreme left side of quadrant No. 4 illustrates the parallel extinction of wollastonite with crossed Nicols. Figure 26, *right*, shows a typical growth of spherulites of wollastonite in green bottle glass.

Figure 27 shows devitrite and wollastonite crystallizing out together in flint glass; the wollastonite, in this case, was the primary phase and the devitrite,

[14] G. W. Morey, "Devitrification of Soda-Lime-Silica Glasses," *Jour. Amer. Ceram. Soc.*, **13** [10] 683–713 (1930).

* See Silverman, p. 383 of footnote 13 (*a*).

† See Bellière, footnote 6.

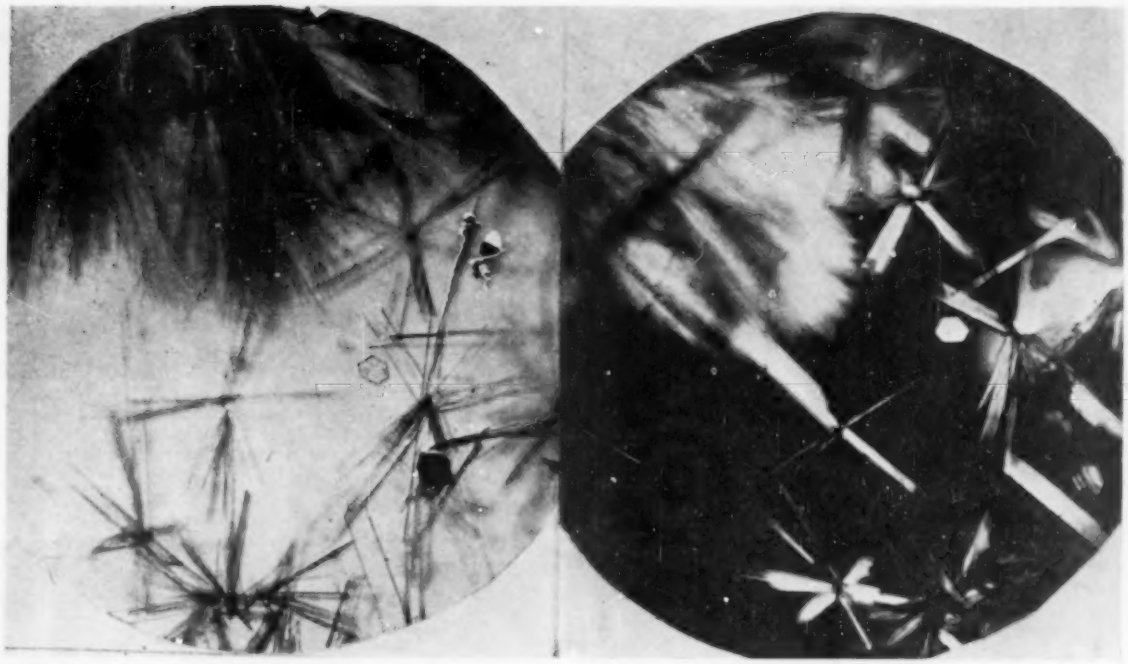

FIG. 27.—Flint glass showing crystallization of devitrite and wollastonite together with wollastonite as primary phase; sample from cooled glass in forehearth; *left*, transmitted light × 100; *right*, crossed Nicols × 100.

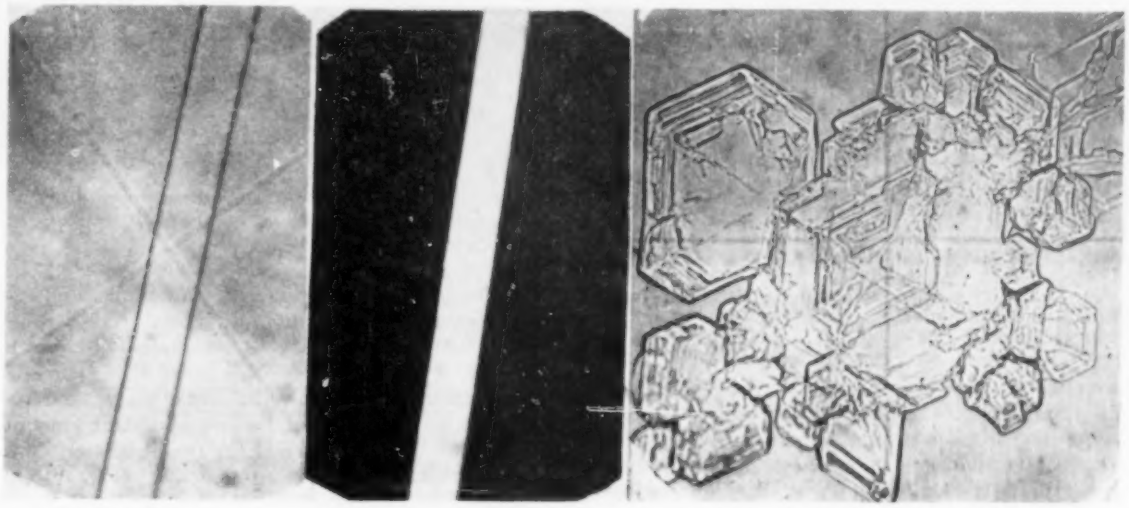

FIG. 28.—*Left* and *middle:* Sample from side wall of green beverage bottle showing large well-developed crystal of wollastonite; *left*, transmitted light × 80; *middle*, crossed Nicols × 80; *right:* sample from bottom of amber beverage bottle showing typical hexagonal crystals of pseudowollastonite, transmitted light × 80.

the secondary phase, but the wollastonite does not represent decomposition of the devitrite.

Figure 28, *left*, shows an unusually large and well-developed crystal of wollastonite; Fig. 28, *middle*, with crossed Nicols shows how wollastonite transmits light in the inclined position. A good example of pseudowollastonite is shown in Fig. 28, *right;* these crystals are typical hexagonal plates; they resemble some forms of tridymite and also corundum but they can easily be distinguished by their index.

(*D*) *Diopside:* Diopside ($CaO \cdot MgO \cdot 2SiO_2$) is another interesting devitrification product. It occurs in glasses where magnesia is present in large enough amount to permit it to form. The exact amount of magnesia necessary for its formation is open to question owing to the influence of other fluxes in the batch. It has been known, however, to form in glasses containing dolomitic limestone with a magnesia content slightly over 3%.

Diopside devitrification has been considered by some

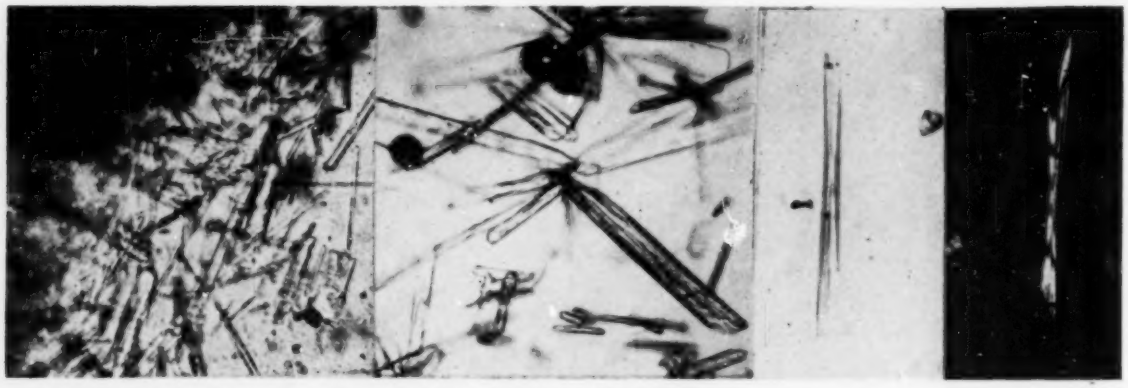

FIG. 29.—*Left:* Diopside crystals from bottom of operating forehearth melting flint glass, transmitted light × 225; *middle:* diopside crystals from flint glass surface of laboratory crucible, transmitted light × 100; *right:* green glass with hollow crystal diopside showing transmission of light in parallel position (*light portion*, transmitted light × 100; *dark portion*, crossed Nicols × 100).

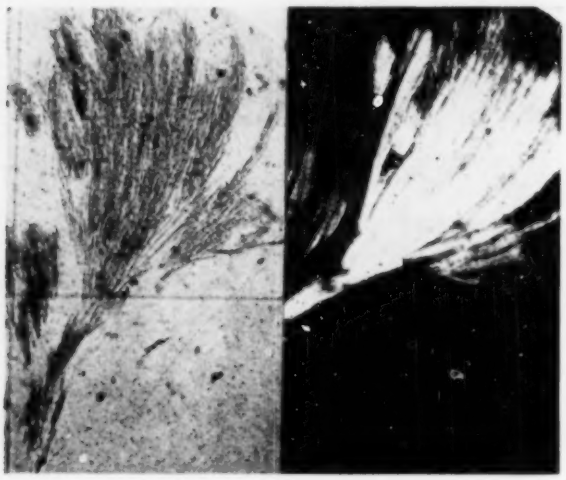

FIG. 30.—Fan-shaped devitrite crystallization from side wall of amber bottle; *left*, transmitted light × 100; *right*, crossed Nicols × 100.

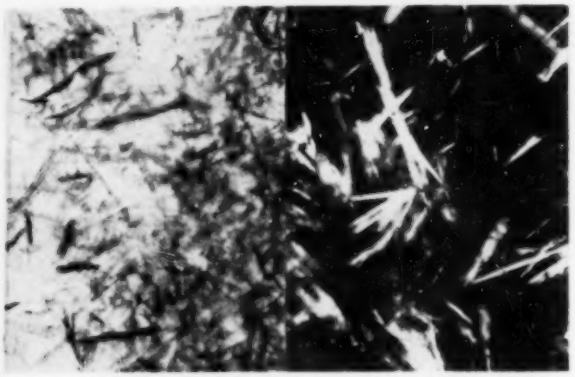

FIG. 31.—Devitrite and cristobalite from an operating Owens pot melting flint glass; *left*, transmitted light × 100; *right*, crossed Nicols × 100.

investigators as a rather rare occurrence. The author finds that it is not uncommon and has encountered it frequently. It forms as prismatic crystals scattered through the glass, as solid masses, or as spherulites, and it can be recognized easily by its high birefringence and extinction angle.

Diopside extinguishes obliquely between 37° to 44° on crystals parallel to the c-axis, a characteristic that serves to differentiate it and beta-wollastonite, which has parallel extinction. It is biaxial positive. Under certain conditions, diopside crystals form with hollow centers (these phenomena have been disucssed by Holland and Preston*).

Figure 29, *left*, shows a solid mass of diopside crystals with those at the edge pulling out and beginning to float away in the glass. These crystals formed in the bottom of an operating forehearth. By insulating the forehearth and raising the temperature above the liquidus, they were eliminated. An analysis of a solid portion of the mass of diopside crystals was SiO_2 75.73, Al_2O_3 0.61, CaO 6.12, MgO 4.20, alkalis 12.61, and BaO 0.46%.

Figure 29, *middle*, shows an area of glass taken from a laboratory crucible that had an abundant amount of diopside. Figure 29, *right* (in two sections), shows a single crystal of diopside with a hollow center; it polarizes light under crossed Nicols when parallel to the cross hairs (reference to Fig. 26, *left*, shows that wollastonite does not do this).

(*E*) *Devitrite:* Devitrite ($Na_2O \cdot 3CaO \cdot 6SiO_2$) occurs as long lathlike crystals, sometimes appearing almost needlelike. It devitrifies in spherulites, in masses, or scattered through the glass, and these often take a characteristic radiating, feathery, fanlike growth. At temperatures above 1050°C., under the proper conditions, it will sometimes decompose into a glassy phase and wollastonite. Devitrite is quite easy to confuse with wollastonite. The writer finds, in general, that it can be distinguished by its somewhat finer crystal growth and feathery habit. When this identification fails, an index determination will separate the two

* See Holland and Preston, p. 94 of footnote 7.

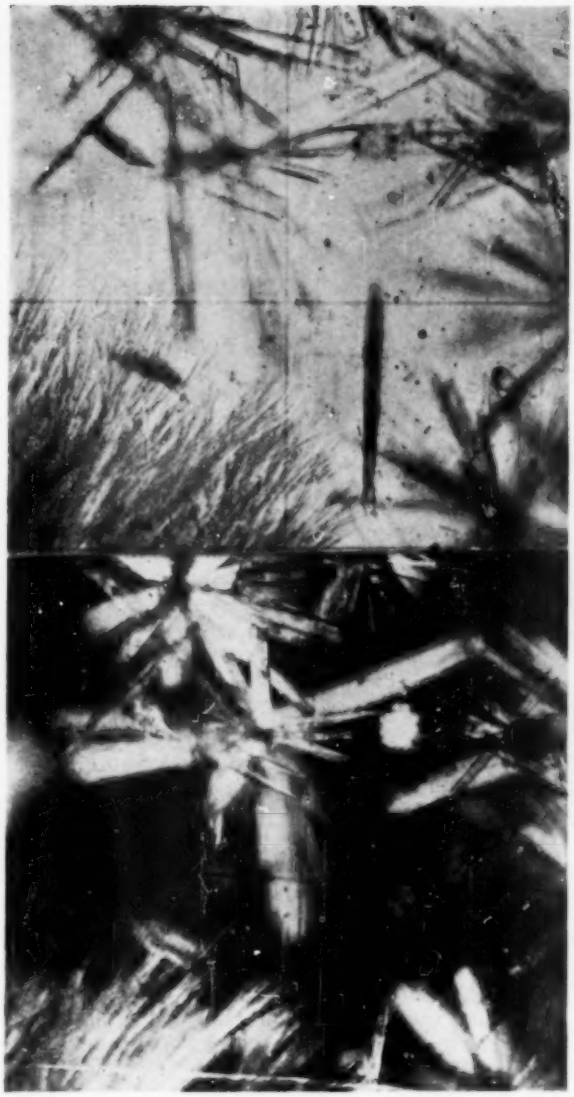

FIG. 32.—Devitrite and beta-wollastonite together from refiner of emerald green furnace; *upper*, transmitted light × 100; *lower*, crossed Nicols × 100.

minerals because devitrite has a much lower index. It is biaxial positive with positive elongation and parallel extinction.

Devitrite is commonly found associated with wollastonite or with cristobalite and tridymite.

Figure 30, *left*, shows a radiating fan of devitrite taken from the side wall of an amber bottle; Fig. 30, *right*, was meant to show the parallel extinction of devitrite by extinguishing the large portion of this fan in the upper right-hand quadrant. The slide, unfortunately, was jostled and was so turned that the crossed-Nicol photograph shows the small fan over the cross hairs partially extinguished; the large fan is in enough of an oblique position to transmit light fully.

Figure 31 shows a solid mass of cristobalite and devitrite mixed in flint glass as taken from an operating

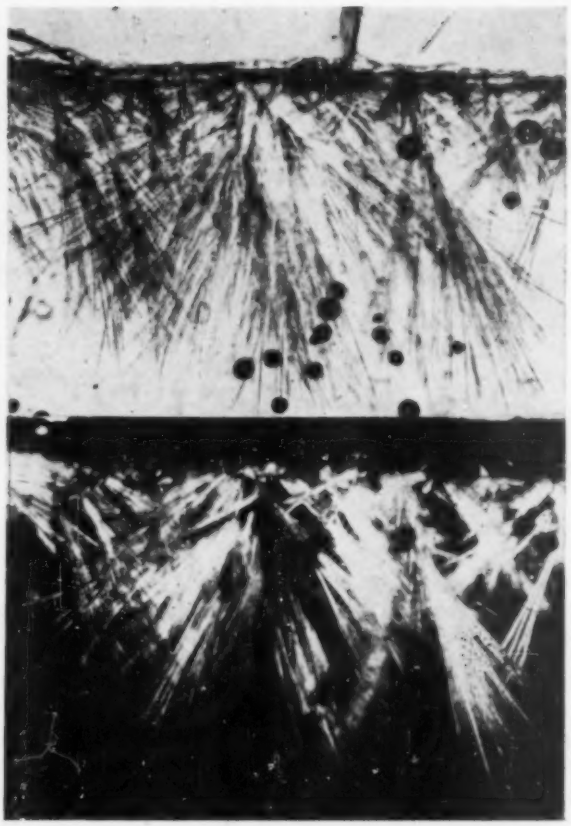

FIG. 33.—Devitrite at surface of laboratory-prepared specimen of flint glass; *upper*, transmitted light × 100; *lower*, crossed Nicols × 100.

Owens pot. The feathery bundles of devitrite (*left*) are almost indistinguishable in the mass of cristobalite, but the devitrite (*right*) becomes quite visible with crossed Nicols.

Figure 32 shows devitrite and wollastonite together, taken from the refiner of an operating emerald green furnace. The fine needle-like crystals in the lower left-hand quadrant (*upper*) are devitrite, and the broader ribbon-like groups are beta-wollastonite.

Figure 33 shows a sample of surface devitrification of devitrite taken from a laboratory-prepared crucible; the crystals start at the outer surface and extend downward into the body of the glass.

Figure 34 shows to what extent the crystals have thinned out $^1/_2$ in. below the surface shown in Fig. 33. The numerous bubbles seen in these sections are characteristic of a great many laboratory-prepared specimens.

(5) Miscellaneous Stones

The stones to be discussed in this section could very well have been included under the discussion on cullet. These few stones, however, are different in that their origin is considered to be within the furnace itself rather than in the cullet.

(*A*) *Sulfate Stones:* Sulfate stones may occur from

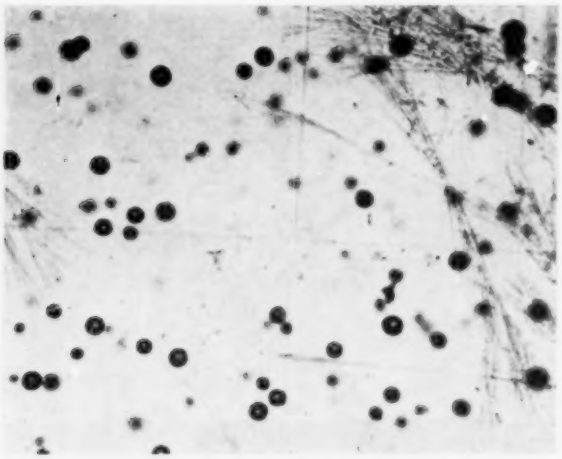

FIG. 34.—Thinning out of devitrification of devitrite $^1/_2$ inch from surface of sample shown in Fig. 33; transmitted light × 100.

the use of saltcake in the batch or, when no saltcake is used, by the condensation of the sulfates on the cooler parts of the furnace refiner and forehearth. Sulfur dioxide in the furnace may be formed from the type of fuel used, whether it is coal, gas, or oil.

Under proper conditions, which appear to be the presence of oxygen, the sodium oxide in the glass or the volatile vapors form sulfates with the sulfur dioxide. By some such complex process, carbonates are formed in a similar way, and the resultant blob scab or boil may be sodium sulfate, sodium carbonate, or a mixture of both. Such stones may occur as large patches of white material or as characteristic blisters. Sometimes they have no crystalline structure or they may be strongly crystalline. Microscopic examination usually identifies this material, but it is easy to check because it is soluble in water and a simple qualitative test can be made.

The best cure for sulfate scum is to use fuels as low in sulfur as possible and to maintain reducing furnace fires. Good hot glass is also an aid, especially in alcoves and forehearths as it delays the solid formation of sulfates. Such crusts on the upper structure keep falling into the glass and are a nuisance. If a solid film of saltcake forms on the refiner or forehearth, the quickest way to get rid of it is to cool the surface of the glass and to ladle it off. If the film forms only in the forehearth, it can sometimes be tapped off the surface while in a liquid state.

Figures 35 and 36 show examples of typical sulfate scabs found in the side walls of flint bottles.

(*B*) *Metal Stones:* A source of iron blobs may occur from the ironwork supporting and binding the furnace. Many supporting channels protrude far enough into the refractory walls of the furnace so that when the refractory wears away, portions of the iron supports themselves are attacked by the furnace vapors and temperatures and melt away. Machine parts also may drop into the glass, particularly in Owens operation, and cause trouble.

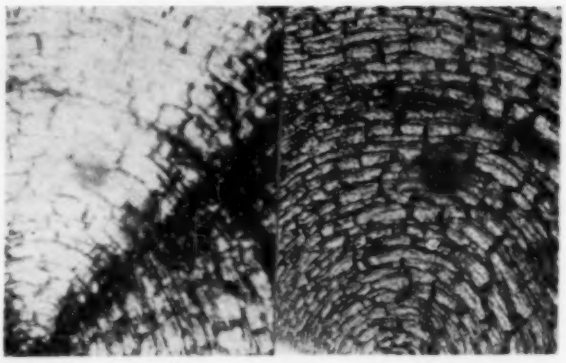

FIG. 35.—Sulfate blisters in flint bottles; *left*, transmitted light × 80; *right*, crossed Nicols, × 80.

Such stones are definitely not classed in importance with the preceding types, but they are quite common and deserve mention. It is sometimes important to distinguish whether the metal stone involved is nickel, lead, iron, or steel. Chemical facilities, however, are not always at hand for metallurgical checks. Of the metals encountered in a glass furnace, nickel is magnetic and lead and aluminum are not. Iron may or may not be magnetic, depending on whether it is austenitic (austenitic iron is not magnetic).

An iron stone can quickly be distinguished from the nickel by putting dilute nitric acid on it and precipitating the resultant liquid with ammonia; any iron that is present will precipitate out as ferric hydroxide, which is a brown precipitate.

It is often valuable to know whether the iron is coming from furnace steel or if it is cast iron from the machine. In this case, the piece of glass containing the stone should be ground until a small flat area of the metal stone is exposed, which should be given a metallurgical polish suitable for etching.

The stone is etched* by immersing and rinsing off in Nital, which is a 2% solution of HNO_3 in commercial alcohol. When the desired contrast is secured, it is examined in reflected light under a microscope. The presence of ferrite grains alone (carbon-free iron) is generally indicative of steel; cast iron would show some graphite flakes; and pearlite can be present in either case. (Austenitic iron would naturally show austenite grains.) Figure 37, *left*, shows an etched stone with large well-defined ferrite grains. Figure 37, *middle* and *right*, shows the futility of simply grinding down a metal stone and trying to test it by ordinary methods; meaningless blobs are obtained and the optical properties cannot be determined.

(*C*) *Blisters and Coloring Material:* Streamers or ribbons of what seems to be a solid white material occasionally appear in ware made by Owens operation. A close examination often reveals this material to be only a stream of small entrapped air blisters, caused by the folding in of air in the glass stream from trough

* The writer is indebted to N. Waterbury, Owens-Illinois Glass Co., for all metallurgical tests and information.

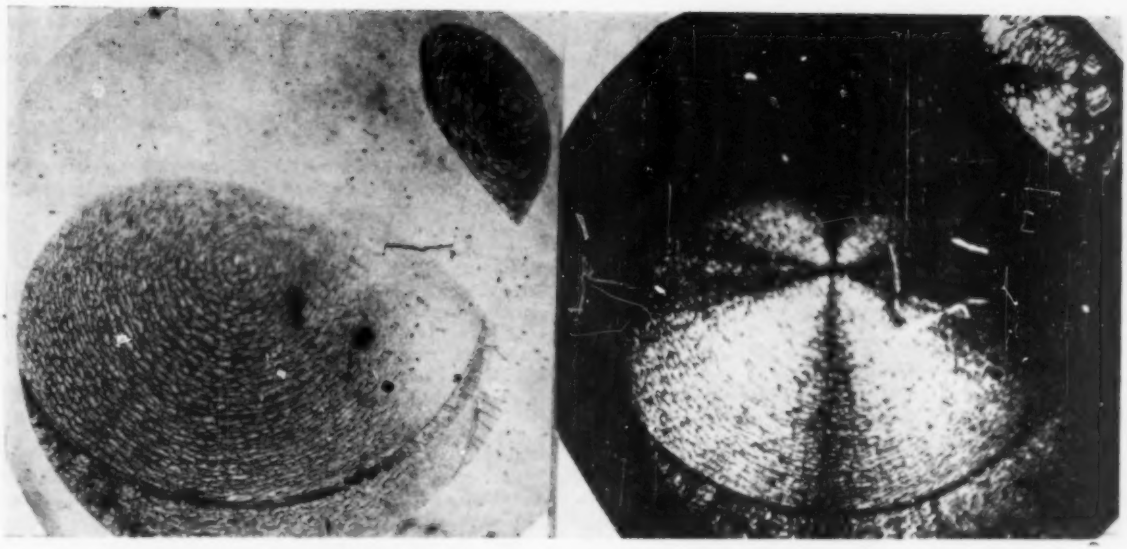

FIG. 36.—Sulfate blisters in flint bottles; *left*, transmitted light × 80; *right*, crossed Nicols × 80.

FIG. 37.—*Left:* Ferrite development brought out in iron stone by acid etching, reflected light × 100; *middle* and *right:* metal stones, transmitted light × 125.

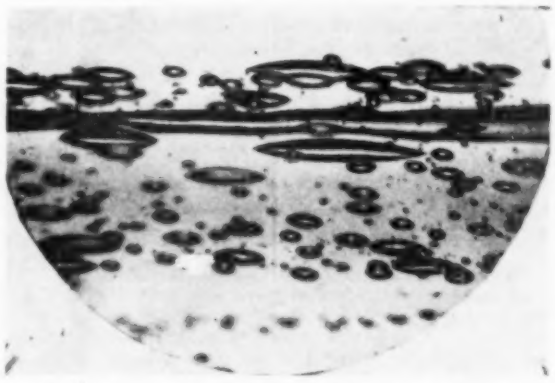

FIG. 38.—Stream of entrapped air bubbles, transmitted light × 125.

to pot. Figure 38 shows a stream of such blisters or air bubbles.

Coarse-grained or damp coloring materials used in batches for colored glasses may cause trouble. These cases are rare, but each presents an individual problem, and an intelligent diagnosis by the operator always results in the proper steps being taken to clear up the difficulty.

V. Conclusions

The entire field of glass stones is of sufficient importance and scope that more time and attention should be given to it by each individual plant. Unfortunately, it is difficult to convince a works manager, for example, that, by peering through a microscope, the identification of a stray bit of dendrite as a certain material can affect his financial ledger. It is just as true that such identification may not tip the ledger profitably unless this information is used correctly. The mere identification of a stone as such will not in itself decrease the loss; everyone concerned on the job must apply the information obtained. The complete story of each stone problem is necessary and, more important, a true record should be kept of the remedies tried and the results secured. This record will help the person who identifies the stones to know whether his diagnosis has been correct and what procedure to follow if the same situation

occurs again. Changes too often are made on a furnace and the stones will disappear, but no one has determined a definite source of the stones so that when the same perplexing problem arises later on, the same confusion occurs.

The identification of glass stones, although not the most difficult task, is still far from being the cut-and-tried proposition that textbooks may indicate. The petrographer, for example, should never scorn aid in identification from other sources, such as by chemical analysis or by any other means available. Sometimes he will need all of them.

Bibliography

1. A. F. Rogers and P. F. Kerr, Optical Mineralogy. 2d ed., pp. 79–376. McGraw-Hill Book Co., Inc., New York, 1942. 390 pp.
2. Eric Preston and W. E. S. Turner, "Fundamental Studies of Glassmelting Process, Effect of Particle Size and Temperature on Rate of Glass Formation of Pure Soda-Lime-Silica Glass," *Jour. Soc. Glass Tech.*, **23** [103] 124–38 (1940); *Ceram. Abs.*, **22** [4] 89 (1941).
3. J. H. Partridge, "Effect of Gases on Commercial Glass Containing Lead Oxide," *Jour. Soc. Glass Tech.*, **16**, 121–30 (1932); *Ceram. Abs.*, **11** [12] 611 (1932).
4. C. N. Fenner, "Relations Between Tridymite and Cristobalite," *Jour. Soc. Glass Tech.*, **3**, 116–25 (1919).
5. C. J. Peddle, "Development of Various Types of Glass, VI–IX," *ibid.*, **4**, 299–366 (1920); abstracted in *Jour. Amer. Ceram. Soc.* (*Ceram. Abs.*), **3** [8] 681–82 (1920).
6. C. J. Peddle, "Development of Various Types of Glass: X, Comparison of Alkali-Lime-Silica and Alkali-Lead Oxide-Silica Glasses," *Jour. Soc. Glass Tech.*, **5**, 72–106 (1921).
7. Eric Preston, "Crystallization Relationship of Soda-Lime-Magnesia-Silica Glass as Used for Drawn Sheet and Process of Devitrification," *Jour. Soc. Glass Tech.*, **24** [104] 139–58 (1940); *Ceram. Abs.*, **20** [4] 88 (1941).
8. Herbert Insley, "Petrographic Microscope as Instrument for Glass Technologist," *Jour. Amer. Ceram. Soc.*, **11** [11] 812–28 (1928).
9. C. W. Parmelee and A. J. Monack, "Devitrification of Glass: (1) Relative Stabilities of Different Glasses, (2) Time-Temperature Curves of Visible Devitrification, (3) Proposed Classification of Glasses," *Jour. Soc. Glass Tech.*, **13**, 322–36 (1929); *Ceram. Abs.*, **9** [7] 512 (1930).
10. W. R. Lester, "Influence of Silica Stones on Strength of Glass Containers," *Glass Ind.*, **23** [12] 461–62 (1942); *Ceram. Abs.*, **22** [2] 31 (1943).
11. H. Jebsen-Marwedel, "Chemistry of Glass-Furnace Construction: I, Slagging Processes Above Metal Line," *Glastech. Ber.*, **15** [4] 131–36 (1937); translated in *Glass Ind.*, **18** [9] 304 (1937); *Ceram. Abs.*, **17** [5] 176 (1938).
12. Percy Haller, "Some Random Notes on Tank Practice," *Glass*, **16** [1] 8–15 (1939).
13. Marcel Bellière, "Formation of Cristobalite as Octahedra in Devitrified Glass," *Glass Ind.*, **15** [11] 239–40 (1934); *Ceram. Abs.*, **14** [2] 34 (1935).
14. N. W. Taylor and C.-Y. Lin, "Effect of Various Catalysts on Conversion of Quartz to Cristobalite and Tridymite at High Temperatures," *Jour. Amer. Ceram. Soc.*, **24** [2] 57–63 (1941).
15. N. L. Bowen and J. W. Greig, "System Al_2O_3–SiO_2," *ibid.*, **7** [4] 238–54 (1924); correction, [5] 410.
16. International Critical Tables, Vol. I, 1926.
17. A. Dietzel, "Methods for Investigation of Little Stones and Knobs in Glass," *Sprechsaal*, **66** [49] 837–39; [50] 853–56; [51] 867–69 (1933); *Ceram. Abs.*, **13** [5] 115 (1934).

General Engineering Laboratory
Owens-Illinois Glass Company
Alton, Illinois

MECHANICS OF ENAMEL ADHERENCE: XVI, INFLUENCE OF MANGANESE DIOXIDE ON METAL PRECIPITATION AT GROUND COAT-IRON INTERFACE*

By R. M. King

Abstract

The influence of manganese oxide alone and in combination with cobalt and nickel oxides on metal precipitation in ground coats has been studied. The previously developed electrical-resistance method was used. Manganese dioxide present alone was not effective in precipitating metal. The results on the indirect influence of manganese dioxide in combination with cobalt and nickel oxides are not significant.

I. Introduction

In the two preceding papers of this series,[1] data were presented showing the influence of cobalt and nickel oxides on metal precipitation in fired ground coats as determined by an electrical-resistance method. This paper offers data to show the influence of manganese dioxide on the phenomenon of metal precipitation.

Referring to the work of Bernard,[2] who also studied the decomposition of solid solutions of MnO and FeO, the following pertinent statements are cited:

> FeO and MnO mixtures of low MnO content . . . . . are much more stable at low temperatures than FeO. A mixture containing 5% MnO and kept for several hours at 800°C. . . . . does not show any decomposition. When one increases the content of manganese protoxide in the solid solution he notices the irreversible formation of more and more . . . . . magnetite . . . . . at any reheating temperature.

Bernard does not report the formation of iron from any composition of FeO and MnO. On the basis of his

* Presented at the Forty-Sixth Annual Meeting, The American Ceramic Society, April 4, 1944 (Enamel Division). Received April 4, 1944.

[1] (*a*) R. M. King, "Mechanics of Enamel Adherence: XIV, Role of Cobalt Oxide in Metal and Oxide Precipitation During Ground-Coat Firing Cycle and Determination of Temperature and Time Intervals of Precipitation," *Jour. Amer. Ceram. Soc.*, **26** [2] 41–48 (1943); (*b*) XV, Influence of Cobalt and Nickel Oxides on Metal Precipitation at Ground Coat-Iron Interface" *ibid.*, [10] 358–59.

[2] Jaques Bernard, "Étude de la Decomposition du Protoxide de Fer et de ses Solutions Solides," *Ann. Chim.*, [Series 11], **12** [1] 5–92 (1939).

work, therefore, manganese oxide would not be expected to aid in the precipitation of iron in ground coats.

Very little information is found in the literature regarding the role of manganese dioxide in ground coats. Markert[3] states that there is no difference in the adherence to steel of ground coats containing manganese dioxide as compared with enamels using cobalt oxide alone or in combination with other oxides. He also indicates that ground coats containing manganese dioxide have higher maturing temperatures, other factors being equal, and that it reduces the coefficient of expansion.

Howe[4] reported that "cobalt was essential in producing adherence in a ground-coat enamel while manganese and nickel improved adherence over a wider firing range."

TABLE I

SIGNIFICANT DATA

Composition No.	Composition (%)	R_1* (ohms)	C†	R_2‡ (ohms) (avg.)	Standard deviation	S.D.§ factor
1	1.22 MnO_2	10^5		9×10^4		
2	0.46 Co_3O_4 0.15 Ni_2O_3	10^5	2	6.5	3.28	
						0.6
3	0.46 Co_3O_4 0.15 Ni_2O_3 0.61 MnO_2	10^2	1	5.5	0.66	
4	0.44 Co_3O_4 0.15 Ni_2O_3	10^5	2	20.6	20.0	
						0.06
5	0.44 Co_3O_4 0.15 Ni_2O_3 0.59 MnO_2	3×10^2	1	20.1	9.7	

* R_1, order of maximum resistance during first cooling period.

† C, serial number of cooling period during which decrease in resistance began.

‡ R_2, resistance after complete cooling; values are averages of not less than 4 determinations.

§ S.D. factor, statistical factor indicating whether difference of means is significant (should be 2 or greater if significant)

II. Experimental Procedure

(1) Enamels and Method Employed

The base frits used were the same as those listed in part XIV.[1(a)] Each composition tested contained 50% of soft and 50% of hard frit and manganese dioxide, cobalt oxide, and nickel oxide as indicated in Table I. Lower percentages of cobalt and nickel oxides than used in previous studies were added to render the enamels more sensitive to any possible influence of manganese oxide, that is, the resistance values obtained by the use of 0.65% of cobalt plus nickel oxides, for example, were so low that it was thought that any possible changes brought about by manganese dioxide would not be distinguishable.

The apparatus and procedure were the same as those employed in paper XV.[1(b)]

III. Results

(1) Discussion of Data

Significant data are shown in Table I. It has been pointed out that lower percentages of cobalt and nickel oxides were used in this study to render the resistance response more sensitive to manganese dioxide. Compositions were selected therefore which showed considerable variation from test to test. The rather wide standard deviations indicate such variations.

The results obtained with composition No. 1 are sufficient to prove that manganese dioxide did not bring about any observable precipitation of metal. No difference between these results and those obtained previously[1(a)] with a white ground coat was noted. It will be observed also that this composition contained 1.22% MnO_2 and that marked metal precipitation was obtained from the other compositions in Table I, some of which contained an amount as low as 0.59% of total cobalt and nickel oxides.

It was thought, however, that manganese dioxide added along with cobalt and nickel oxides might have some indirect influence, such as that of hardening or softening the enamel or oxidation. The paired compositions Nos. 2 and 3 and Nos. 4 and 5 were designed and tested to reveal any possible influence of this nature. On comparing the deviations from the means of compositions (No. 3 with No. 2 and No. 5 with No. 4), it might be concluded that manganese dioxide aids in smoothing out variations from test to test, but differences in precipitation are not significant.

IV. Conclusions

The presence of manganese oxide alone in ground coats did not bring about a detectable precipitation of metal even when available in double the minimum effective percentages of cobalt and nickel oxides. This statement is in harmony with the work of Bernard[2] on the decomposition of solid solutions of manganese and iron protoxides.

Manganese oxide in combination with cobalt and nickel oxides showed no significant indirect influence on metal precipitation.

DEPARTMENT OF CERAMIC ENGINEERING
OHIO STATE UNIVERSITY
COLUMBUS 10, OHIO

[3] F. S. Markert, "Function of Manganese Dioxide in Ground Coat," *Enamelist*, **3** [1] 26 (1925); Enamel Bibliography, p. 207. The American Ceramic Society, publisher, May, 1929.

[4] E. E. Howe and R. L. Fellows, "Effect of Manganese, Nickel, and Cobalt Oxide on Adherence and Reboiling Properties of Ground-Coat Enamels," *Jour. Amer. Ceram. Soc.*, **20** [10] 319–24 (1937).

OBSERVATIONS INDICATING ABSENCE OF PLASTIC FLOW IN GLASS COATING ON STEEL*

By W. G. Martin and F. W. Lauck

Abstract

Steel rings were glass coated, and some were split at one point immediately and others one or two years later. Identical movement of the rings caused by compressive forces in the glass indicated that no plastic flow takes place in the glass. The compressive forces were calculated and found to be of the general order of 10,000 lb. per sq. in. The method of calculation is described.

I. Introduction

A number of investigators have reported evidence that glass may deform very slowly at room temperature over a long period of time.[1] The theory has been advanced that very old stained-glass church windows derive some of their exceptional beauty from the fact that plastic flow of the glass has resulted in a slight thickening of the lower portion, thereby causing attractive and pleasing light effects. Whether or not this is true, there have been other accounts of the flow of glass in forms which are much more obvious. For example, a flat glass plate was used to cover the corrugated bottom of a trough employed for hydraulic experiments. The apparatus was placed in a storeroom and, after ten or fifteen years, it was noted that the glass had begun to conform noticeably to the corrugations upon which it lay.

The authors are aware of only one paper dealing directly with this subject. In 1930, Spencer[2] concluded that glass rods and tubes do not assume a permanent bend under their own weight. The same writer, however, did produce 9 mm. of permanent deflection in glass tubing 1 meter long, which was held by force in a curved position for six years.

It then occurred to the writers that glass coats on steel might undergo plastic flow over a period of time because of the compressive stresses which are known to be imposed upon the glass by the steel. That glass fused to steel is under compression is well known, and Rosenberg and Langerman[3] have published a paper on this subject.

The present authors had a different interest, however, inasmuch as they wished to know whether or not any change in the compressive stresses would take place over a period of time and whether the compressive stresses were high enough to justify an expectation of plastic flow at room temperature.

II. Experimental Procedure

In order to ascertain whether or not the glass coatings would flow at room temperature, it was decided to glass coat thin steel rings on the outside. Any flow, or thickening, of the glass would result in a decrease of the compression stresses in the glass. These stresses would be in proportion to the amount of contraction of the rings after they were cut through by sawing. Any change in the stresses after varying aging time and corresponding change in contraction of the ring would indicate plastic flow of the glass.

A number of rings, 1 in. wide, were cut from a length of seamless tubing of 3-in. outside diameter and 0.037-in. wall thickness. Some of these rings were coated with glass on the outside only, while several uncoated rings were fired with the same time-temperature cycles in order to determine the nature of the stresses in the steel itself. Two coats of glass, or two firing cycles, were applied to all rings except those which were not annealed. The glass thickness was 0.010 in.

The glass-coated rings incidentally were cut through in one place and again partially through about $^3/_8$ in. away from the first cut so that one end could be bent down out of the way of the other end to allow free contraction of the ring.

III. Results

Table I presents a condensed review of the various conditions and results obtained (see also Fig. 1).

It will be noted that uncoated, annealed rings expanded $^9/_{32}$ in. when cut, which indicates that a considerable amount of stress was locked in the steel as a result of the manufacturing operations. The annealed, uncoated rings expanded only $^1/_{16}$ in., so that obviously the stresses in the metal had been considerably reduced as a result of the annealing effect of the firing cycles.

All the rings, moreover, that were coated with glass on the outside surface contracted $^5/_{32}$ in. when cut. In other words, for rings having identical treatment, the contraction was the same whether they were cut soon after glass lining or following a varying period of aging. The writers conclude that there was no plastic flow in the glass, even during the period of two years and three months.

A check on these findings was obtained by taking additional rings from the same length of tubing and glass coating them on the inside only. When these rings were cut, they expanded $^9/_{32}$ in. Because the annealed, uncoated rings normally expanded $^1/_{16}$ in. and rings

* Presented at the Forty-Sixth Annual Meeting, The American Ceramic Society, Pittsburgh, Pa., April 5, 1944 (Enamel Division). Received April 5, 1944.

[1] "Manufacture of Optical Glass and of Optical Systems," Document No. 2037, U. S. Ordnance Dept.

[2] S. D. Spencer, "Do Glass Rods and Tubes Bend under Their Own Weight?" *Nature*, **125**, 707 (1930).

[3] J. E. Rosenberg and A. Langerman, "Method and Apparatus for Studying Physical Properties of Vitreous Enamels on Steel," *Jour. Amer. Ceram. Soc.*, **19** [3] 86–90 (1936).

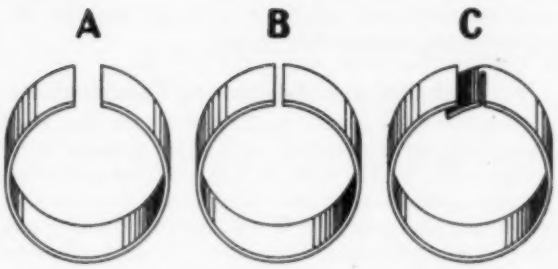

FIG. 1.—Three steel rings, each given different treatment, cut to show stress conditions; (*A*) no glass coating, no heat-treatment, $^{9}/_{32}$-in. expansion; (*B*) no glass coating but fired same as for glass coating, $^{1}/_{16}$-in. expansion; (*C*) two coats of glass, outside only, $^{5}/_{32}$-in. contraction.

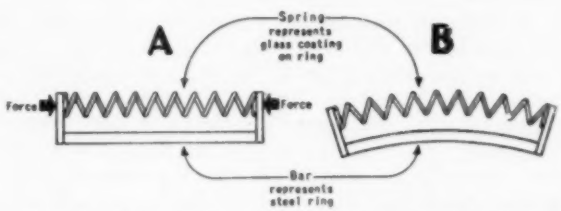

FIG. 2.—Compression spring and bar couple analogous to relationship of glass coating on steel rings in experiments; (*A*) bar and spring held in equilibrium by two forces; relationship analogous to situation in glass-coated ring before it is cut; (*B*) with forces removed, spring balances the resistance of bar to further bending; relationship analogous to situation in glass-coated ring after it is cut.

with glass on the outside contracted only $^{5}/_{32}$ in., the net movement may be considered to be $^{7}/_{32}$ in. This result checks with the movement of the rings glass coated on the inside only, inasmuch as the $^{9}/_{32}$-in. expansion of these rings should be corrected by subtracting the $^{1}/_{16}$-in. expansion of the rings which were annealed but not glass coated.

IV. Discussion of Results and Calculations

After obtaining the foregoing results, which clearly indicated that no plastic flow took place in the glass coating, the authors cast about for some obvious explanation. No plastic flow in the glass would be expected unless there was a considerable amount of stress present in the glass to cause it to flow. To gain some knowledge concerning the magnitude of the stresses in the glass, a check was made on the studies on the stresses in steel tubing.[4] The investigators in this field found that the amount of opening or closing of a ring of metal cut from the tubing may be used in a formula to determine the stress in the steel prior to cutting through the ring (formula (1)).

Since this formula relates the movement of the ends of a cut steel ring to the stresses in the ring, the formula may also be used to calculate the stresses introduced in the steel when the glass is permitted to bend the steel ring after it is cut.

[4] W. M. Frame, Casing Settling Depths Not Assured by Physical Properties of Steel. National Supply Co., American Petroleum Inst., May, 1938.

TABLE I

CONDITIONS AND RESULTS OBTAINED ON TEST SAMPLES

Treatment of rings	No. of each type	Movement of cut ends allowing for width of saw cut (in.)	Time between glass lining and cutting
		(Expansion)	
Not glass coated Not annealed	4	$^{9}/_{32}$	
Not glass coated Annealed by 2 firing cycles to 1600°F.	4	$^{1}/_{16}$	
Two glass coats Inner surface only	2	$^{9}/_{32}$	2 hr.
		(Contraction)	
Two glass coats Outer surface only	4	$^{5}/_{32}$	2 hr.
Two glass coats Outer surface only	5	$^{5}/_{32}$	12 mo.
Two glass coats Outer surface only	5	$^{5}/_{32}$	2 yr. and 3 mo.

Figure 2 shows an analogy to the situation in the glass-coated rings. For purposes of analysis, it is more simple to think of the glass as a compression spring not fastened to the steel except at the ends. Before cutting the ring, the glass coat cannot bend the steel (the situation is shown in the view on the left (Fig. 2 (*A*)). When the rigidity of the ring is destroyed by cutting through it at one point in its circumference, the glass coat is strong enough to bend the steel. This is represented in the view on the right (Fig. 2 (*B*)). It should be noted that in Fig. 2 (*B*) the spring is still under considerable compression and is in balance with the resistance of the steel to bending.

From formula (1), the moment in the steel is found to be 1.95 in.-lb. when the ring is contracted $^{5}/_{32}$ in. This moment is produced by a load in the glass coat acting on a moment arm 0.0235 in. long, the distance from the neutral axis of the steel to the center of the glass coat.

The load, or force, in the glass coat must then be equal to the moment in the steel divided by the moment arm, which is 83 lb.

The section area of the glass is approximately 0.01 sq. in., and the stress in the glass must be 8300 lb. per sq. in. when the ring is contracted $^{5}/_{32}$ in.

The contraction of the ring, however, lowered the stress in the glass, and it was desirable to know the stress in the glass before the ring was cut.

Figure 3 shows an analysis of a method of arriving at the change in length of a unit length of glass when the ring expands or contracts. It is based on the assumption that when the steel bends the neutral axis does not change in length. Thus $L_{1S} = L_{2S}$. If L_{1S} is 1 in. and since R_1, R_2, and d can be measured or calculated in inches, then ϵ (the elongation in in. per in.) can be calculated and is 2.6×10^{-4} in. per in.

$$M = \frac{2aEI}{4\pi R^3} \qquad (1)$$

M = moment of forces (in.-lb.).
a = opening or closing of ring (in.).
E = modulus of elasticity of steel (30×10^6 lb./sq. in.).
I = moment of inertia (in. to 4th power).
R = radius of ring to center line of steel.

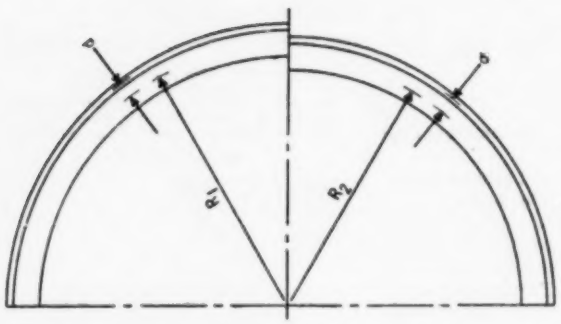

FIG. 3.—Method of calculating change in unit length of glass coating when ring contracts. L_{1G} = glass length before cutting; L_{2G} = glass length after cutting; L_{1S} = steel length before cutting; L_{2S} = steel length after cutting; ϵ = elongation of glass (in./in.); d = distance from center line of glass to center line of steel; R_1 = radius to center line of steel before cutting; R_2 = radius to center line of steel after cutting.

$$\frac{L_{1G}}{L_{1S}} = \frac{R_1 + d}{R_1} \text{ and } \frac{L_{2G}}{L_{2S}} = \frac{R_2 + d}{R_2}$$

$$L_{1S} = L_{2S} = 1 \text{ in.}$$

$$\epsilon = \frac{R_2 + d}{R_2} - \frac{R_1 + d}{R_1} = \frac{d(R_1 - R_2)}{R_1 \cdot R_2}$$

This value of ϵ may be used in formula (2).

$$S = E\epsilon \qquad (2)$$

S = stress (lb./sq. in.).
E = modulus of elasticity 10,000,000 lb./sq. in.
S = 2600 lb./sq. in..

This 2600 lb. per sq. in. is the decrease in stress in the glass as the ring contracts after being cut. Since the stress in the glass after contraction was calculated to be 8300 lb. per sq. in., the sum of these figures, 10,900 lb. per sq. in., is the calculated stress in the glass before the rings were cut.

This value, 10,900 lb. per sq. in., is only about 10% of the compression strength of glass; percentage-wise, it is not impressive. Spencer,[2] however, obtained 9 cm. permanent bend in a 1-meter bar supported at the ends and weighted in the center. The data he furnished indicate an imposed stress of the order of 3000 lb. per sq. in. This stress is roughly 25% of the probable tensile strength[5] of the glass and is therefore greater percentage-wise than the compressive stresses found in the glass-coated rings.[6] The stress, however, in the glass on the steel rings was about three times the stress in the glass tube which suffered plastic flow. Therefore, it appears that the absence of plastic flow must be ascribed to some other restraining influence, perhaps derived from the very small thickness dimension and the relatively large ratio of surface to mass.

[5] (*a*) A. I. Andrews, Enamels, p. 360. Twin City Printing Co., Champaign, Ill., 1935. 410 pp.; *Ceram. Abs.*, **14** [7] 158 (1935).
(*b*) H. Hovestadt, Jena Glass and Its Scientific and Industrial Applications, p. 149. Tr. by J. D. Everett and Alice Everett. Macmillan Co., London, 1902.

[6] C. W. Parmelee and D. T. Shaw, "Effect of Additions of CaO and MgO on Enamel Glasses," *Jour. Amer. Ceram. Soc.*, **13** [7] 498–508 (1930).

V. Technical and Mathematical Considerations

Concerning the stresses in the glass on the steel rings, the authors were interested only in obtaining accuracy within 10% of the true values. To have obtained greater accuracy than this would have increased the amount of work many fold without contributing anything to the knowledge of the behavior of the glass under the conditions described. It was useful, however, to know whether the stresses were low or high. Accordingly in the calculations, the value of 10×10^7 lb. per sq. in. was used for the modulus of elasticity, although it is known that the true modulus for various glasses may be 5 to 10% lower or higher than this figure.

In order to simplify the calculations, the bending moment in the glass itself was neglected, and it was assumed that the stresses in the glass were in straight compression only. A further assumption that the stresses act at the center line of glass and steel is reasonably accurate, especially since the glass was only 0.010 in. thick. Owing to the bending moments mentioned and to the variations in coefficient of expansion, this assumption is not theoretically correct.

Formula (1), $M = 2aEI/4\pi R^2$, used to calculate the moment in the steel after the rings were cut, was developed for use where steel rings expand and contract because of internal stresses in the steel itself. It is believed that no great errors are involved when the formula is used for glass-coated rings instead of plain steel rings.

The measurements of the expansion or contraction of the rings were made with an accuracy within $^1/_{64}$ in. In view of the purpose of the measurements and because of the other assumptions and the practical impossibility of accurate values of all the factors involved, this accuracy of measurement was considered to be satisfactory.

VI. Summary

(1) Equal contraction of glass-coated steel rings cut immediately after firing and those cut one and two years later indicates no plastic flow of the glass coating.

(2) Calculations indicate a compressive stress of 10,900 lb. per sq. in. in the glass coating.

(3) No definite explanation is advanced for the absence of plastic flow under such stress values except the suggestion that the cross-section dimensions of the glass and relatively large surface area may account for restraining forces.

Acknowledgment

The authors wish to acknowledge with thanks the assistance of W. R. Kepler and C. Scudder of the Engineering Department in the mathematical work; the collaboration of W. W. Higgins of the Ceramic Laboratory for the glass coating of the rings; the graphic presentation and general assistance of J. Dilot of the Advertising Department; and the facilities extended by the A. O. Smith Corporation.

A. O. SMITH CORPORATION
MILWAUKEE 1, WISCONSIN

ENAMEL BIBLIOGRAPHY AND ABSTRACTS

1929 to 1939, Inclusive, with Subject and Coauthor Indexes

Edited and Published by

The American Ceramic Society, Incorporated

2525 North High Street, Columbus 2, Ohio

1944 Price $5.00

There are approximately 5000 references in this work. Of these, 359 are from original papers published in the *Journal* and *Bulletin of The American Ceramic Society*. There are also 300 United States patents, 94 British, 92 German, and 79 patents from other countries, all having appeared in *Ceramic Abstracts*.

The Bibliography covers the entire scope of world writers in the porcelain enamel field. Practically all of these references in this book have been previously published in *Ceramic Abstracts*.

The present volume was preceded by the first edition of Bibliography and Abstracts of the Literature on Enamels compiled by Robert D. Landrum and Herbert D. Carter, and was edited and published in May, 1929.

THESE VOLUMES COVER THE WRITTEN HISTORY OF COMMERCIAL ENAMELING ON METALS

(1944)

47th

Annual Meeting

THE AMERICAN CERAMIC SOCIETY, APRIL 15-19, 1945

Hotel Statler, Buffalo, N. Y.

A Victory Conference

A Readjustment Conference

AN "Imagineering" for Postwar

Seven Divisions Meeting Simultaneously

Design • Enamel • Glass
Materials and Equipment • Refractories
Structural Clay Products • White Wares

Institute of Ceramic Engineers
Ceramic Educational Council
Ceramic Camera Club

Dr. Clarence Samuel Ross Will Deliver the Edward Orton, Jr., Fellow Lecture

OFFICIAL PERSONNEL OF DIVISIONS, 1944–1945

	Design	Enamel	Glass	Materials and Equipment	Refractories	Structural Clay Products	White Wares
Trustee	W. A. Weldon	R. L. Fellows	J. S. Gregorius	J. E. Eagle	J. B. Austin	Frederick Heath, Jr.	J. W. Hepplewhite
Chairman	W. A. Weldon	H. D. Carter	K. C. Lyon	J. R. Kauffman	W. R. Kerr	R. L. Stone	J. W. Whittemore
Vice-Chairman	Theodore Lenchner	W. W. Higgins	Louis Navias	J. F. Day	S. M. Swain	E. F. Theobald	R. M. Campbell
Secretary	Myrtle M. French	D. G. Moore	S. R. Scholes	V. J. Roehm	E. E. Callinan	R. L. Ferguson	C. M. Lambe, Jr.
Division Nominations	Alice A. Ayars K. E. Smith	F. R. Porter M. J. Bahnsen Karl Kautz	R. A. Miller W. R. Lester L. W. Peterson	J. F. McMahon E. M. Rupp	J. B. Austin C. L. Thompson G. J. Easter	A. P. Potts R. L. Ferguson C. F. Wiseman	J. R. Beam F. C. Henderson R. Russell, Jr.
Papers and Program	C. M. Harder Vincent Broomhall H. L. Moody	W. W. Higgins	Louis Navias	W. E. Dougherty E. W. Emrich J. S. Breitenstein	C. A. Freeman W. S. Debenham B. L. Dorsey	A. C. Jackson H. L. Winburn J. G. Seanor	E. P. McNamara
Membership	W. J. Harr Herbert Tepping G. W. Fichter C. K. Williams	A. I. Andrews J. F. Hunt F. A. Petersen	F .V. Tooley R. R. Shively	V. V. Kelsey	L. C. Hewitt F. E. Lobaugh H. M. Parkhurst E. M. Sarraf	C. F. Tefft L. R. Whitaker H. C. Plummer J. H. Isenhour	A. A. Wells
Standards		R. L. Cook W. N. Harrison R. M. King F. A. Petersen B. W. King, Jr.	Members are Comm. C-14, A.S.T.M.	R. C. Meeker	Members are Comm. C-8, A.S.T.M.	G. R. Robinson	F. P. Hall L. E. Thiess
Research		J. C. Reimers	Alexander Silverman O. G. Burch C. E. Leberknight	R. R. Robinson	E. C. Petrie	G. A. Bole H. C. Plummer	R. Russell, Jr. Glenn Howatt
Classification and Nomenclature	Mrs. J. W. Dixon	G. H. McIntyre E. E. Bryant	E. P. McNamara	J. F. McMahon	C. M. Dodd	E. F. Theobald R. E. Grim	A. S. Watts
Rules	J. P. Thorley	W. A. Deringer O. E. Mulvane	S. R. Scholes	Philip Dressler	S. F. Walton	Howells Fréchette	J. D. Clark
Councillors		D. G. Bennett	R. W. Wampler J. F. Greene	V. V. Kelsey		L. R. Whitaker A. P. Potts	
Exhibitions	Mrs. L. S. Backus		J. E. Frazier				
Industrial Management			C. J. Uhrmann	S. S. Cole	J. L. Crawford	J. C. Peck	
Bibliography	P. E. Cox	J. E. Rosenberg		C. L. Cruikshank			

Officers of Classes

	Institute of Ceramic Engineers	Ceramic Educational Council
Trustee	H. M. Kraner	R. M. Campbell
President	M. F. Beecher	C. M. Dodd
Vice-President	T. A. Klinefelter	A. I. Andrews
Secretary	R. S. Bradley	P. S. Dear

THE AMERICAN CERAMIC SOCIETY TRUSTEES AND OFFICERS FOR 1944–1945

President: E. H. Fritz, Stupakoff Ceramic & Mfg. Co., Latrobe, Pa.
Vice-President: C. Forrest Tefft, The Claycraft Co., Columbus, Ohio
Treasurer: J. D. Sullivan, Battelle Memorial Institute, Columbus 1, Ohio
Secretary-Editor: R. C. Purdy, 2525 North High St., Columbus 2, Ohio
Past-President: C. E. Bales, Ironton Fire Brick Co., Ironton, Ohio
Past-President: L. J. Trostel, General Refractories Co., Baltimore, Md.

TRUSTEES FROM INDUSTRIAL DIVISIONS*

Design: W. A. Weldon, Locke Insulator Corp., Baltimore, Md. (1946)
Enamel: R. L. Fellows, Chicago Vitreous Enamel Product Co., Cicero, Ill. (1946)
Glass: J. S. Gregorius, Pittsburgh Plate Glass Co., Pittsburgh, Pa. (1947)
Materials and Equipment: J. E. Eagle, 6306 20th Ave., Green Meadows, Hyattsville, Md. (1945)
Refractories: J. B. Austin, U. S. Steel Corp., Kearny, N. J. (1946)
Structural Clay Products: Frederick Heath, Jr., Owens-Corning Fiberglas Corp., Toledo, Ohio (1945)
White Wares: J. W. Hepplewhite, Edwin M. Knowles China Co., Newell, W. Va. (1947)
Institute of Ceramic Engineers: H. M. Kraner, Bethlehem Steel Co., Bethlehem, Pa. (1947)
Ceramic Educational Council: R. M. Campbell, New York State College of Ceramics, Alfred, N. Y. (1947)

* Date of expiration of term of office in parentheses.

DIVISION OFFICERS

Design
Chairman: W. A. Weldon, Locke Insulator Corp., Baltimore, Md.
Secretary: Myrtle M. French, Art Institute of Chicago, Chicago, Ill.

Enamel
Chairman: H. D. Carter, Harshaw Chemical Co., Cleveland, Ohio
Secretary: D. G. Moore, National Bureau of Standards, Washington, D. C.

Glass
Chairman: K. C. Lyon, Armstrong Cork Co., Millville, N. J.
Secretary: S. R. Scholes, N. Y. State College of Ceramics, Alfred, N. Y.

Materials and Equipment
Chairman: J. R. Kauffman, Allied Engineering Co., Milltown, N. J.
Secretary: V. J. Roehm, Kentucky Clay Mining Co., Alliance, Ohio

Refractories
Chairman: W. R. Kerr, Armstrong Cork Co., Beaver Falls, Pa.
Secretary: E. E. Callinan, Timken Roller Bearing Co., Timken Steel & Tube Div., Canton, Ohio

Structural Clay Products
Chairman: R. L. Stone, Univ. of North Carolina, Raleigh Unit, Raleigh, N. C.
Secretary: R. L. Ferguson, 730 Stuart Bldg., Lincoln, Nebr.

White Wares
Chairman: J. W. Whittemore, Virginia Polytechnic Institute, Blacksburg, Va.
Secretary: C. M. Lambe, Jr., Univ. of North Carolina, Raleigh Unit, Raleigh, N. C.

OFFICERS OF THE FELLOWS

Dean: R. B. Sosman, U. S. Steel Corp., Kearny, N. J.
Associate Dean: Howells Fréchette, Bureau of Mines, Ottawa, Ontario, Canada.
Secretary-Treasurer: R. M. King, Ohio State University, Columbus, Ohio

INSTITUTE OF CERAMIC ENGINEERS

President: M. F. Beecher, Norton Company, Worcester, Mass.
Vice-President: T. A. Klinefelter, U. S. Bureau of Mines, Tuscaloosa, Ala.
Secretary: R. S. Bradley, A. P. Green Fire Brick Co., Mexico, Mo.

CERAMIC EDUCATIONAL COUNCIL

President: C. M. Dodd, Iowa State College, Ames, Iowa
Vice-President: A. I. Andrews, University of Illinois, Urbana, Ill.
Secretary: Paul S. Dear, Virginia Polytechnic Institute, Blacksburg, Va.

LOCAL SECTIONS

Baltimore-Washington
Chairman: W. R. Lester, Maryland Glass Co., Baltimore, Md.
Secretary: C. B. Shelley, General Refractories Co., Baltimore, Md.

Central Ohio
Chairman: H. J. Orlowski, O.S.U. Engr. Expt. Sta., Columbus, Ohio
Secretary: A. C. Jackson, Claycraft Co., Columbus, Ohio

Chicago
Chairman: Hugo Filippi, Illinois Brick Co., 228 N. LaSalle St., Chicago, Ill.
Secretary: J. J. Svec, Industrial Publications, Inc., 59 E. Van Buren St., Chicago, Ill.

Michigan
Chairman: J. F. Quirk, A C Spark Plug Co., Flint, Mich.
Secretary: W. V. Blake, Macklin Co., Jackson, Mich.

Northern California
President: W. V. Bragdon, California Faience Co., Berkeley, Calif.
Secretary: P. C. Valentine, Del Monte Properties Co., San Francisco, Calif.

Northern Ohio Section
Chairman: E. M. Sarraf, Harbison-Walker Refractories Co., Cleveland 13, Ohio
Secretary: S. M. Swain, North American Refractories Co., Cleveland 14, Ohio

Pacific-Northwest
President: Gordon Adderson, Gladding, McBean & Co., Renton, Wash.
Secretary: K. G. Skinner, Bureau of Mines, Univ. of Washington, Seattle, Wash.

Pittsburgh
Chairman: W. C. Rueckel, Koppers Co., Pittsburgh, Pa.
Secretary: J. W. Jordan, Mellon Institute, Pittsburgh, Pa.

Southern California
Chairman: R. F. Evans, Gladding McBean, & Co. Glendale, Calif.
Secretary: Guy Wurtsbaugh, Pacific Clay Products, Los Angeles, Calif.

St. Louis
Chairman: H. H. Hanna, Pittsburgh Plate Glass Co., Crystal City, Mo.
Secretary: J. H. Ivery, Hydraulic Press Brick Co., St. Louis, Mo.

Upstate New York
Chairman: M. H. Berns, Electro Refractories & Alloys Corp., Buffalo, N. Y.
Secretary: E. E. Kunzman, Titanium Alloy Mfg. Co., Niagara Falls, N. Y.

THE JOURNAL OF THE AMERICAN CERAMIC SOCIETY, NOVEMBER 1, 1944 Vol. 27, No. 11, pp. 317-354 (1944)